②

NAVAL POSTGRADUATE SCHOOL

Monterey, California

AD-A261 747

DTIC
ELECTE
MAR 15 1993
S E D

THESIS

INTRODUCTION TO CHAOTIC DYNAMICAL SYSTEMS

by

Michael A. Bernhard

December 1992

Thesis Advisor: Ismor Fischer

Approved for public release; distribution is unlimited

93-05286

93 3 12 03

Unclassified

security classification of this page

REPORT DOCUMENTATION PAGE

1a Report Security Classification Unclassified		1b Restrictive Markings	
2a Security Classification Authority		3 Distribution Availability of Report Approved for public release; distribution is unlimited.	
2b Declassification Downgrading Schedule			
4 Performing Organization Report Number(s)		5 Monitoring Organization Report Number(s)	
6a Name of Performing Organization Naval Postgraduate School	6b Office Symbol (if applicable) MA	7a Name of Monitoring Organization Naval Postgraduate School	
6c Address (city, state, and ZIP code) Monterey, CA 93943-5000		7b Address (city, state, and ZIP code) Monterey, CA 93943-5000	
8a Name of Funding Sponsoring Organization	8b Office Symbol (if applicable)	9 Procurement Instrument Identification Number	
8c Address (city, state, and ZIP code)		10 Source of Funding Numbers Program Element No / Project No / Task No / Work Unit Accession No	

11 Title (include security classification) INTRODUCTION TO CHAOTIC DYNAMICAL SYSTEMS

12 Personal Author(s) Michael A. Bernhard

13a Type of Report	13b Time Covered	14 Date of Report (year, month, day)	15 Page Count
Master's Thesis	From To	December 1992	78

16 Supplementary Notation The views expressed in this thesis are those of the author and do not reflect the official policy or position of the Department of Defense or the U.S. Government.

17 Cosati Codes			18 Subject Terms (continue on reverse if necessary and identify by block number)
Field	Group	Subgroup	word processing, Script, GML, text processing.

19 Abstract (continue on reverse if necessary and identify by block number)

The emerging discipline known as "chaos theory" is a relatively new field of study with a diverse range of applications (economics, biology, meteorology, etc.). Despite this, there is not as yet a universally accepted definition for "chaos" as it applies to general dynamical systems. Various approaches range from topological methods of a qualitative description, to physical notions of randomness, information, and entropy in ergodic theory, to the development of computational definitions and algorithms designed to obtain quantitative information.

This thesis develops some of the current definitions and discusses several quantitative measures of chaos. It is intended to stimulate the interest of undergraduate and graduate students and is accessible to those with a knowledge of advanced calculus and ordinary differential equations. In covering chaos for continuous systems it serves as a complement to the work done by Philip Beaver [Ref. 1], which details chaotic dynamics for discrete systems.

20 Distribution Availability of Abstract ☒ unclassified unlimited ☐ same as report ☐ DTIC users	21 Abstract Security Classification Unclassified	
22a Name of Responsible Individual Ismor Fischer	22b Telephone (include Area code) (408) 646-2206	22c Office Symbol MA Fi

DD FORM 1473,84 MAR 83 APR edition may be used until exhausted
All other editions are obsolete

security classification of this page

Unclassified

Introduction to
Chaotic Dynamical Systems

by

Michael A. Bernhard
Lieutenant, United States Navy
B.S., University of Illinois, 1987

Submitted in partial fulfillment of the
requirements for the degree of

MASTER OF SCIENCE IN APPLIED MATHEMATICS

from the

NAVAL POSTGRADUATE SCHOOL
December 1992

Author: Michael A. Bernhard

Michael A. Bernhard

Approved by:

Ismor Fischer, Thesis Advisor

Jeffery J. Leader

Jeffery J. Leader, Second Reader

Richard Franke

Richard Franke, Chairman,
Department of Mathematics

ABSTRACT

The emerging discipline known as "chaos theory" is a relatively new field of study with a diverse range of applications (economics, biology, meteorology, etc.). Despite this, there is not as yet a universally accepted definition for "chaos" as it applies to general dynamical systems. Various approaches range from topological methods of a qualitative description, to physical notions of randomness, information, and entropy in ergodic theory, to the development of computational definitions and algorithms designed to obtain quantitative information.

This thesis develops some of the current definitions and discusses several quantitative measures of chaos. It is intended to stimulate the interest of undergraduate and graduate students and is accessible to those with a knowledge of advanced calculus and ordinary differential equations. In covering chaos for continuous systems it serves as a complement to the work done by Philip Beaver [Ref. 1], which details chaotic dynamics for discrete systems.

TABLE OF CONTENTS

I. INTRODUCTION

In recent years, new topological methods stemming from work done in the late nineteenth and early twentieth century by French mathematician and physicist Henri Poincaré have been applied to the classical "analytical" theory of ordinary differential equations. The powerful discipline which has emerged has come to be known as "dynamical systems theory," with applications not only to continuous, but to discrete systems as well, such as recursive or iterative feedback loops. One result of these methods is the ability to detect, describe, and measure the elusive phenomenon of "chaos."

Simply put "chaos" is the occurrence of behavior that appears "random" in a deterministic dynamical system, that is, a system that changes in time governed at least in principle by certain known physical or mathematical laws. It is a phenomenon that is *intrinsic* to many dynamical systems, and not due to external influences such as "noise." Examples are wide-ranging, and include the motion of the planets, turbulent fluid flow, and population fluctuations. Additional applications have come from many fields of study, such as astronomy, biology, chemistry, ecology, economics, geology, mathematics, medicine, physics, and some social sciences, as well as various engineering disciplines. In addition, many of these ideas have captured the public imagination, resulting in a great number of popular expositions. In recent years, various attempts have been made to codify these important concepts, and develop a rigorous unifying theory of "chaotic dynamics."

This thesis introduces the reader to some of the methods of determining the presence of "chaos" in continuous systems as well as measuring it quantitatively. The information presented should be accessible to those with a knowledge of advanced calculus and ordinary differential equations. To this end, the proofs of presented theorems which exceed this knowledge are referenced for the interested reader.

II. BASIC CONCEPTS

A. SYSTEMS OF FIRST ORDER DIFFERENTIAL EQUATIONS

We begin with a general system of first order ordinary differential equations expressed in the vector form

$$x' = f(x,t). \tag{1}$$

with $x' = \frac{dx}{dt}$ for $x = [x_1, x_2, \dots, x_n] \in \mathbb{R}^n$, and $f = [f_1, f_2, \dots, f_n] \in \mathbb{R}^n$, where each f_i, $i = 1, 2, \dots, n$ assigns a real scalar value to every point $x \in \mathbb{R}^n$ and time $t \in \mathbb{R}$. Hence f_i: $\mathbb{R}^{n+1} \to \mathbb{R}$, and so f: $\mathbb{R}^{n+1} \to \mathbb{R}^n$. For example, with n = 3, equation (1) is equivalent to

$$\begin{bmatrix} x_1' \\ x_2' \\ x_3' \end{bmatrix} = \begin{bmatrix} f_1(x_1, x_2, x_3, t) \\ f_2(x_1, x_2, x_3, t) \\ f_3(x_1, x_2, x_3, t) \end{bmatrix}. \tag{2}$$

Whenever possible vectors will be written in column form, however we may take the liberty, as was done for the vectors x and f, to write them as rows. The vector function f in equations (1) and (2) is defined as a **vector field** in $\mathbb{R}^n$. In a **non-autonomous** system, f depends explicitly on the variable t. An **autonomous** system is one in which f has no explicit time dependence; in this case equation (1) can be written as

$$x' = f(x), \tag{3}$$

where f: $\mathbb{R}^n \to \mathbb{R}^n$ for $x \in \mathbb{R}^n$.

It should be noted that higher order differential equations can be written as a system of first order differential equations. For example, consider the second order differential equation

$$y'' + 5y' + 4y = 0. \tag{4}$$

With new variables defined by

$$x = \begin{bmatrix} x_1 \\ x_2 \end{bmatrix} = \begin{bmatrix} y \\ y' \end{bmatrix}. \tag{5}$$

we have

$$x' = \begin{bmatrix} x_1' \\ x_2' \end{bmatrix} = \begin{bmatrix} y' \\ y'' \end{bmatrix} = \begin{bmatrix} 0y + 1y' \\ -4y - 5y' \end{bmatrix}, \tag{6}$$

i.e., the original equation (4) is equivalent to the 2×2 system

$$x' = Ax, \tag{7}$$

$$\text{with } A = \begin{bmatrix} 0 & 1 \\ -4 & -5 \end{bmatrix}. \tag{8}$$

For methods of converting higher order differential equations to first order systems see Borrelli-Coleman [Ref. 2].

The general form of a **linear** system of differential equations is

$$\begin{bmatrix} x_1' \\ \cdot \\ \cdot \\ \cdot \\ x_n' \end{bmatrix} = \begin{bmatrix} a_{11}(t)x_1 + \ldots + a_{1n}(t)x_n + F_1(t) \\ \cdot \\ \cdot \\ \cdot \\ a_{n1}(t)x_1 + \ldots + a_{nn}(t)x_n + F_n(t) \end{bmatrix} \tag{9}$$

where $F_i: \mathbb{R} \to \mathbb{R}$ and each $a_{ij}: \mathbb{R} \to \mathbb{R}$, i = 1,...,n, j = 1,...,n. Equivalently,

$$x' = A(t)x + F(t) \tag{10}$$

where $A = (a_{ij}(t))_{\substack{i=1,\ldots,n \\ j=1,\ldots,n}}$ and $F: \mathbb{R} \to \mathbb{R}^n$ is given by $F = [F_1, \ldots, F_n]$. If the linear system is autonomous, then a_{ij} and F_i are constants. A **nonlinear** system of differential equations is one which is not linear.

If the linear system is such that the functions F_i are identically zero, then the system is said to be **homogeneous** and can be written in the form

$$x' = A(t)x. \tag{11}$$

$A(t)$ is a matrix consisting of the same a_{ij} as in equation (9). Again, if the linear homogeneous system is autonomous, then the matrix A is constant, as in (7) and (8).

It is also true that a non-autonomous system such as (1) can be written as an autonomous one. This is done by considering t as a dependent variable, increasing the size of the problem from n to n + 1:

$$\begin{aligned} x' &= f(x,t) \\ t' &= 1 \end{aligned} \tag{12}$$

is equivalent to

$$y' = g(y) \tag{13}$$

with

$$y = \begin{bmatrix} x \\ t \end{bmatrix} \in \mathbb{R}^{n+1} \text{ and } g\colon \mathbb{R}^{n+1} \to \mathbb{R}^{n+1} \text{ given by } g(y) = \begin{bmatrix} f(y) \\ 1 \end{bmatrix}. \tag{14}$$

Since any system can be written as an autonomous one, it will be assumed without loss of generality that the system is autonomous unless specified otherwise.

The general solution to a system of differential equations - denoted $\phi_t(x)$ - is called a **flow** and equation (3) implies that $\phi_t'(x) = f(\phi_t(x))$. As an example, $\phi_t(x)$ for a third order system (i.e., n = 3) takes the form

$$\phi_t(x) = \begin{bmatrix} x_1(t) \\ x_2(t) \\ x_3(t) \end{bmatrix}, \tag{15}$$

and defines a family of solutions or **integral curves.** An **initial condition** for the system (3) typically has the form $x(t_0) = x_0$, and physically prescribes a point $x_0 \in \mathbb{R}^n$ through which the flow passes at time $t = t_0$. Under certain conditions according to the basic local existence and uniqueness theorem of ordinary differential equations (see Coddington-Levinson [Ref. 3]), this flow is uniquely determined, so that $\phi_{t_0}(x) = x_0$. Often, without loss of generality, time $t_0 = 0$ is chosen for the initial condition; then $\phi_0(x) = x_0$.

B. ASYMPTOTIC BEHAVIOR OF FLOWS

One of the objectives of the modern theory of differential equations, or dynamical systems, is to describe the global rather than just the local behavior of flows. To this end, we introduce a number of definitions and then provide several examples to illustrate them.

The **forward orbit** of a flow $\phi_t(x)$ based at a point $x \in \mathbb{R}^n$ is defined as $\{\phi_t(x): 0 \leq t < \infty\}$. The **backward orbit** of $\phi_t(x)$ is defined as $\{\phi_t(x): -\infty < t \leq 0\}$. The **full orbit** of a flow $\phi_t(x)$ is defined as $\{\phi_t(x): -\infty < t < \infty\}$. We remark that an orbit is also sometimes referred to as a **trajectory**.

A point $p \in \mathbb{R}^n$ is an **equilibrium** or **stationary point** if $x_0 = p$ implies that $\phi_t(x) = p$ for all $t > 0$. These correspond to critical points of $x(t)$, and so may be found by setting $x' = 0$ in equation (3). A **periodic orbit** of **period T** is defined as a set $\{\phi_t(x): 0 \leq t < \mathrm{T}\}$ for some $\mathrm{T} \geq 0$ such that $\phi_{\mathrm{T}}(x) = x$. If $\phi_t(x) \neq x$ for any $0 < t < \mathrm{T}$, then T is the **fundamental, minimal** or **prime** period for $\phi_t(x)$. The flow of an equilibrium point can be viewed as a periodic orbit of period zero. A **quasi-periodic orbit** is an orbit that is not periodic, but which can be written as the sum of "incommensurate" periodic orbits. As an example, the flow

$$\phi_t(x) = \cos 2t + \cos \sqrt{2}\, t \tag{16}$$

defines a quasi-periodic orbit. It is written as a sum of periodic orbits, but is not itself periodic since 2 and $\sqrt{2}$ are incommensurate (i.e., $k_1 2 + k_2\sqrt{2} \neq 0$ for any k_1, k_2 integers, both not equal to zero).

Equilibrium points and points of a periodic flow can be viewed collectively as a single set of points. These sets of points are specific examples of what will now be defined as an invariant set. An **invariant set** Λ of a flow is a set such that $\phi_t(\Lambda) = \Lambda$, where we define $\phi_t(\Lambda) = \bigcup_{x \in \Lambda} \phi_t(x)$.

A closed invariant set is **stable** if for every $\varepsilon > 0$, there exists a $\delta > 0$, such that $\|x - \Lambda\| < \delta$ implies that $\|\phi_t(x) - \Lambda\| < \varepsilon$ for all $t > 0$ (i.e., a flow which starts at a point close to Λ, will stay close to Λ). Here ' $\| \, \|$ ' is the standard Euclidean distance in $\mathbb{R}^n$, and $\|x - \Lambda\|$ is defined as the greatest lower bound of $\|x - y\|$ for all $y \in \Lambda$. A closed invariant set Λ is **asymptotically stable** if it is stable and if there exists a $\delta > 0$, such that $\|x - \Lambda\| < \delta$ implies that $\|\phi_t(x) - \Lambda\| \to 0$ as $t \to \infty$. (i.e., a flow which starts at a point close to Λ, will get arbitrarily close to Λ as time advances). A closed invariant set Λ is **unstable** if for every $\varepsilon > 0$ there exists a $\delta > 0$, such that $\|x - \Lambda\| < \delta$ implies that $\|\phi_t(x) - \Lambda\| \to 0$ as $t \to -\infty$ (i.e., a flow which starts at a point close to Λ, will get arbitrarily close to Λ in backward time). We remark that many authors choose to define a closed invariant set as unstable simply if it is not stable. The **limit set** Λ of a flow is defined as the set of all points p such that $\phi_t(x) \to p$ as $t \to \pm\infty$. Note that by construction, Λ is an invariant set.

The following examples of systems of differential equations are provided to illustrate some of the previous definitions.

Example 1 - Population Equation (one dimension)

$$x' = r(M - x)x \tag{17}$$

This differential equation can be used as a simple model of bacteria growth in a Petri dish. The constant r is the positive rate of growth, and M is the positive limiting population constant due to factors such as the size of the Petri dish.

Although this equation can be solved using methods of ordinary differential equations, a qualitative graph of its solutions can be formed using simple analysis. First, note that the constant functions $x = 0$ and $x = M$ are equilibrium solutions of (17). Moreover, if either $x < 0$ or $x > M$, then $x' < 0$, so that x decreases with increasing t.

Likewise if $0 < x < M$, then $x' > 0$, so that x increases with increasing t. Using this analysis the family of solutions is plotted for $t \geq 0$ in Figure 1.

A **phase diagram** is one which eliminates the variable t by projecting the flow curves onto the space $\mathbb{R}^n$ of the x-variables. The direction of flow is shown schematically by arrows. Obviously, since this process results in an n-dimensional portrait, it can only be visualized for n = 1, 2, or 3. The phase diagram for the above population equation is shown in Figure 2.

As observed above, the population equation has two equilibrium points: $x = 0$ and $x = M$. These points can be calculated by setting $x' = 0$ (i.e., $r(M - x)x = 0$). Notice that flows with initial points in $(0, \infty)$ tend toward M as t increases, and away from M as t decreases. This can be seen by either the plot of solutions or the phase diagram. Thus the point M (or more precisely, the closed invariant set $\Lambda = \{M\}$) satisfies the definition of an asymptotically stable equilibrium point, or **sink.** Note also, that flows of points near but not equal to zero tend away from zero as t increases, and tend toward zero as t decreases. Thus zero satisfies the definition of an unstable equilibrium point, or **source.**

Example 2 - Simple Pendulum (two dimensions)

$$\begin{aligned} x_1' &= x_2 \\ x_2' &= \omega^2 \sin x_1 \end{aligned} \tag{18}$$

This system of differential equations describes the motion of a pendulum moving without friction or air resistance. The variable x_1 is the angular displacement of the pendulum from the vertical, x_2 is the angular velocity, and $\omega = g/L$, where g is the gravitational constant and L is length of the pendulum. The process of finding the explicit solution to this system of differential equations is described in Borrelli-Coleman [Ref. 2].

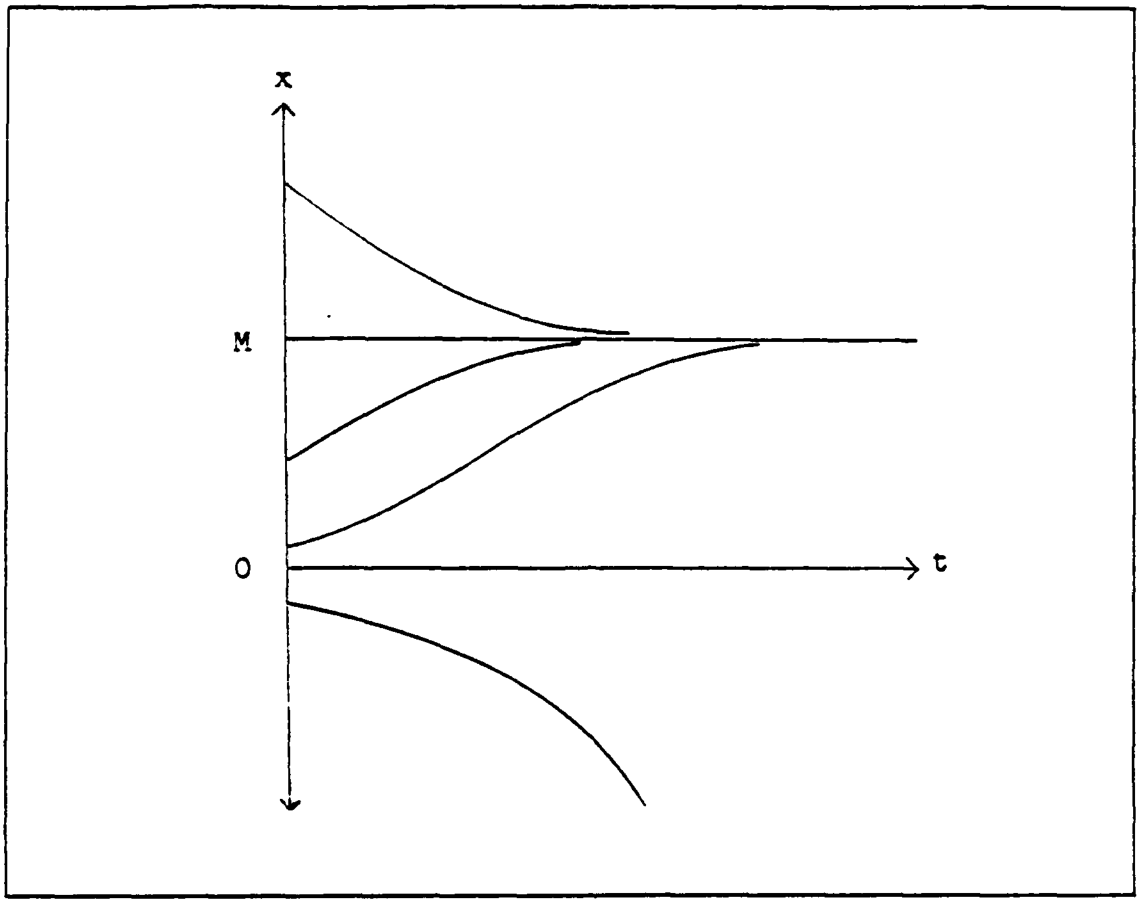

Figure 1. Population Flows

The graph of the family of solutions, if plotted, would be in three dimensions with variables x_1, x_2, t. The plot of the phase diagram is in two dimensions, however, and provides sufficient illustration. The phase diagram is plotted in Figure 3.

The equilibrium points of the simple pendulum are $(n\pi, 0)$ for $n \in \mathbb{Z}$. Again, these can be obtained by setting $x' = 0$ (i.e., $x_1' = 0$ and $x_2' = 0$). Notice that flows with initial conditions near the equilibrium points $(2n\pi, 0)$ for $n \in \mathbb{Z}$ neither converge toward nor diverge from these points, but instead form periodic cycles around them. Hence these equilibrium points are stable but not asymptotically stable, and the associated cycles physically correspond to simple harmonic oscillations of varying amplitudes. The re-

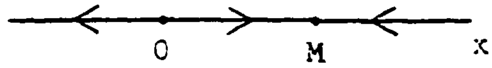

Figure 2. Population Phase Diagram

maining equilibrium points $((2n-1)\pi, 0)$, $n \in \mathbb{Z}$ have flows which converge to and diverge from them. Hence these points are neither stable nor unstable, and are sometimes referred to as **saddle points.**

We remark that an asymptotically stable (respectively, unstable) invariant set for a system can also exist in the form of a **limit cycle** - a simple closed curve γ having the property that nearby trajectories (either interior or exterior to γ) spiral towards (respectively, away from) γ . This phenomenon is typically illustrated by the Van der Pol equation, which models a triode oscillator. The **Poincaré-Bendixson Theorem** essentially asserts that *any* bounded invariant "limit set" of a planar flow is either an equilibrium point, limit cycle, or union of such objects. This fact is in marked contrast to the behavior of discrete flows, and of differentiable flows in dimensions higher than two, where more exotic limit sets, such as "strange attractors," can exist; see Guckenheimer-Holmes [Ref. 4].

C. INVARIANT MANIFOLDS

As stated earlier, a linear homogeneous autonomous system of first order differential equations can be written

$$x' = Ax, \tag{19}$$

where A is a matrix of constants.

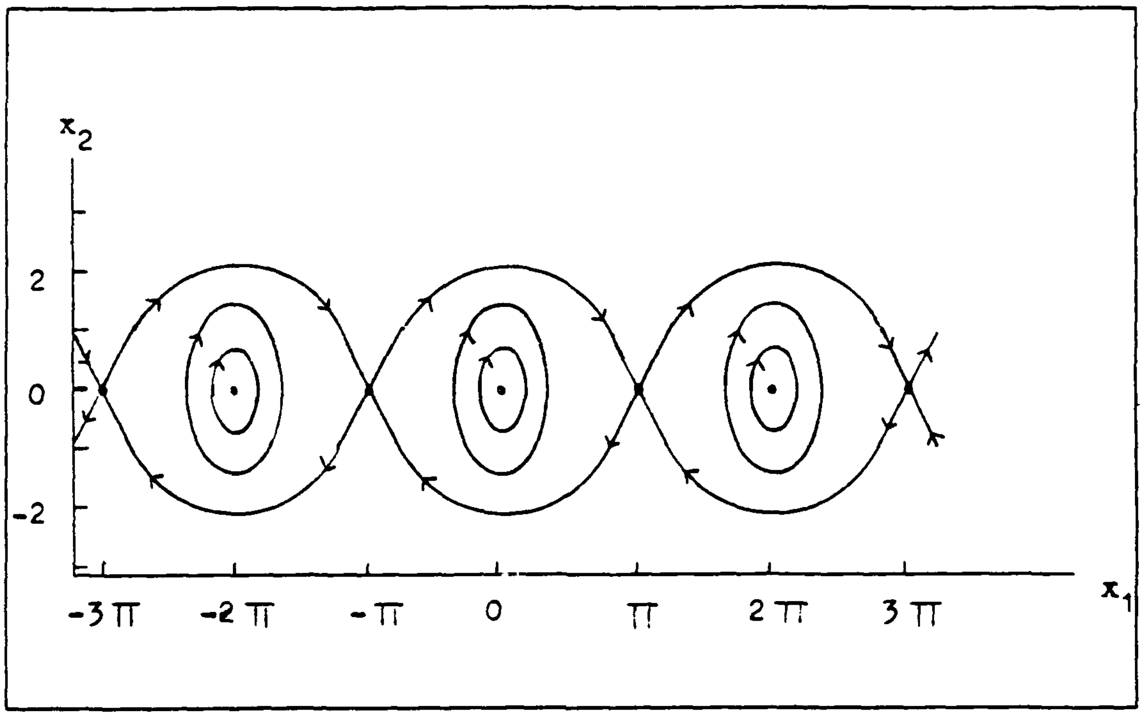

Figure 3. Pendulum Phase Diagram

Theorem 1: If A is n × n and has n independent eigenvectors $[v_1, ..., v_n]$, with corresponding eigenvalues $[\lambda_1, ..., \lambda_n]$, then the family of solutions for (19) is

$$\phi_t(x) = c_1 v_1 e^{\lambda_1 t} + ... + c_n v_n e^{\lambda_n t}, \tag{20}$$

where $c_1, ..., c_n$ are arbitrary constants.

Proof: (Sketch) Note that $x = 0$ is always a solution to the homogeneous system $x' = Ax$. Suppose there exists a nontrivial solution to $x' = Ax$ of the form $x = ve^{\lambda t}$, $v \neq 0$. Substitution of this solution into $x' = Ax$ yields $\lambda v = Av$, thus λ is an eigenvalue of A and v is its associated eigenvector. Due to the linearity of the problem, a linear combination of solutions is a solution, and by a fundamental theorem of ordinary differential equations, *all* solutions must be of this form since we have a full set of linearly independent eigenvectors. The details can be found in Borrelli-Coleman [Ref. 2] and Boyce-DiPrima [Ref. 5].

The c_i are determined once an initial condition $x(0) = x_0$ is given. If a given initial point x_0 lies in the direction of one of the real eigenvectors v_j, then equation (20) becomes

$$\phi_t(x) = c_j v_j e^{\lambda_j t}. \tag{21}$$

Thus the flow through x_0 at $t = 0$ remains in the direction of v_j. If $\lambda_j < 0$, then clearly, $\phi_t(x) \to 0$ as $t \to +\infty$; likewise if $\lambda_j > 0$, then $\phi_t(x) \to \infty$ as $t \to +\infty$. If $\lambda_j = 0$ then (21) reduces to $\phi_t(x) = c_j v_j = x_0$ (i.e., any x_0 in the direction of v_j is an equilibrium point).

For the case of complex eigenvalues $\lambda_j = \alpha + i\beta$ and eigenvectors $v_j = \mathrm{Re}\{v_j\} + i\mathrm{Im}\{v_j\}$, $i = \sqrt{-1}$, the following can be shown. If the initial condition x_0 lies in the plane spanned by $\mathrm{Re}\{v_j\}$ and $\mathrm{Im}\{v_j\}$ then equation (20) can be written in real form as

$$\phi_t(x) = c_{j1} e^{\alpha t} \cos \beta t + c_{j2} e^{\alpha t} \sin \beta t. \tag{22}$$

This implies that the flow remains in the plane spanned by $\mathrm{Re}\{v_j\}$ and $\mathrm{Im}\{v_j\}$ and forms a spiral due to the trigonometric functions, which are oscillating, bounded, and periodic. The direction of the spiral depends on the sign of α. If $\alpha < 0$, the flow spirals in toward the origin. If $\alpha > 0$, the flow spirals out toward infinity. If $\alpha = 0$, the flow forms a periodic cycle about the origin. The constant β determines the rate at which the flow spirals.

It should be noted that for a real matrix A, if λ_j is a complex eigenvalue then its associated eigenvector v_j is complex. In addition, the complex conjugate $\bar{\lambda}_j$ of λ_j is necessarily an eigenvalue and has associated eigenvector $\bar{v}_j$. Note that $\mathrm{Re}\{\lambda_j\}$ is equal to $\mathrm{Re}\{\bar{\lambda}_j\}$.

With these cases in mind, one can divide $\mathbb{R}^n$ into three classes of invariant subspaces called **eigenspaces.** The **stable eigenspace** is defined as $E^s = \text{span}\{v_1, v_2, ..., v_\sigma\}$, where $v_1, v_2, ..., v_\sigma$ are the eigenvectors associated with eigenvalues that have negative real parts with $\sigma = \dim(E^s)$. The **unstable eigenspace** $E^u = \text{span}\{w_1, w_2, ..., w_\upsilon\}$, where $w_1, w_2, ..., w_\upsilon$ are the eigenvectors associated with eigenvalues that have positive real parts, and $\upsilon = \dim(E^u)$. The **center eigenspace** $E^c = \text{span}\{u_1, u_2, ..., u_\gamma\}$, where $u_1, u_2, ..., u_\gamma$ are the eigenvectors associated with eigenvalues that have real parts equal to zero, and $\gamma = \dim(E^c)$. The sum of the dimensions for the eigenspaces is equal to the dimension of the entire space $\mathbb{R}^n$ (i.e., $\sigma + \upsilon + \gamma = n$). Keep in mind that for complex eigenvectors v_i, and $\bar{v}_i$ the spanning vectors for the appropriate eigenspace are $\text{Re}\{v_i\}$ and $\text{Im}\{v_i\}$. Figure 4 is a general phase diagram illustrating the three eigenspaces: a) n = 2, with $\sigma = 1$, $\gamma = 1$, b) n = 2, with $\sigma = 1$, $\upsilon = 1$, and c) n = 3, with $\sigma = 2$, $\upsilon = 1$.

For example, consider $x' = Ax$ where

$$A = \begin{bmatrix} 1 & 1 & 0 & 0 \\ 2 & 2 & 0 & 0 \\ 0 & 0 & 0 & -1 \\ 0 & 0 & 1 & 0 \end{bmatrix}. \tag{23}$$

A has eigenvalues 0, 3, -1+i, -1-i and associated eigenvectors $[1, -1, 0, 0]$, $[1, 2, 0, 0]$, $[0, 0, 0, -1] + i[0, 0, 1, 0]$, $[0, 0, 0, -1] - i[0, 0, 1, 0]$ respectively. Thus $E^s = \text{span}\{[0, 0, 0, -1], [0, 0, 1, 0]\}$, $E^u = \text{span}\{[1, 2, 0, 0]\}$, $E^c = \text{span}\{[1, -1, 0, 0]\}$.

It is always true that zero is an equilibrium point for $x' = Ax$, regardless of A. Note that for A n × n, if the dimension of E^s is equal to n then zero is an asymptotically stable equilibrium point. If the dimension of E^u is equal to n, then zero is an unstable equilibrium point.

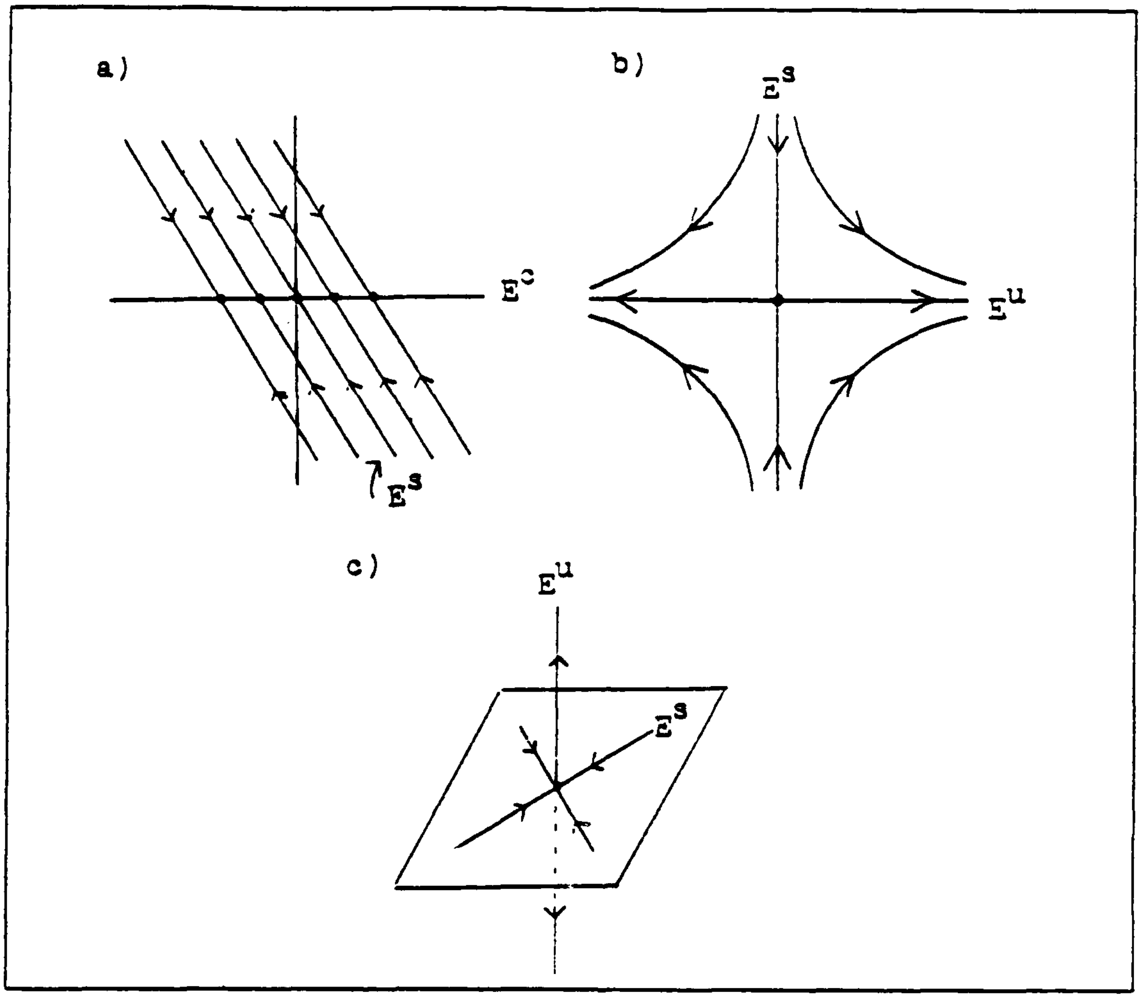

Figure 4. Eigenspaces

The subspaces E^s, E^u, E^c are easily formed when the matrix A has n independent eigenvectors. If the matrix A does not have n independent eigenvectors, the "missing ones" can be constructed using techniques described in Boyce-DiPrima [Ref. 5]. These "generalized" eigenvectors are placed in the appropriate eigenspace depending on the real part of its associated eigenvalue.

For a linear system, flows can be classified rather easily. For a nonlinear system, this is generally not the case. A common method in describing the dynamics of a nonlinear system is to linearize it in a neighborhood of an equilibrium point, so that the analysis above may be applied locally. Given a nonlinear system $x' = f(x)$ and an equilibrium point p, the linearized system is given by

$$x' = Ax, \tag{24}$$

where $A = Df(p) = \left[\frac{\partial f_i}{\partial x_j} \right]_{\substack{i=1,\dots,n \\ j=1,\dots,n}} \Bigg|_{x=p}$ is the Jacobian matrix of f evaluated at p. For example, with $x \in \mathbb{R}^3$,

$$Df(p) = \begin{bmatrix} \frac{\partial f_1}{\partial x_1} & \frac{\partial f_1}{\partial x_2} & \frac{\partial f_1}{\partial x_3} \\ \frac{\partial f_2}{\partial x_1} & \frac{\partial f_2}{\partial x_2} & \frac{\partial f_2}{\partial x_3} \\ \frac{\partial f_3}{\partial x_1} & \frac{\partial f_3}{\partial x_2} & \frac{\partial f_3}{\partial x_3} \end{bmatrix}_{x=p} . \tag{25}$$

We need the following definitions. The **local stable** and **unstable manifolds** of p, $W^s_{loc}(p)$, $W^u_{loc}(p)$ respectively, are defined as follows:

$$W^s_{loc}(p) = \{x \in U: \phi_t(x) \to p \text{ as } t \to +\infty, \text{ and } \phi_t(x) \in U \text{ for all } t \geq 0\} \tag{26}$$

$$W^u_{loc}(p) = \{x \in U: \phi_t(x) \to p \text{ as } t \to -\infty, \text{ and } \phi_t(x) \in U \text{ for all } t \leq 0\} \tag{27}$$

where $U \subset \mathbb{R}^n$ is a neighborhood of p. The **Stable Manifold Theorem** below loosely states that nonlinear systems "resemble" linear systems on a local scale, in the sense that the dynamical roles of the invariant eigenspaces (lines, planes, or "hyperplanes" in higher dimensions) are now played by invariant curves, surfaces, or "manifolds" in general.

Theorem 2: Suppose that $Df(p)$ has no eigenvalues with real part equal to zero. Then there exist unique local stable and unstable manifolds $W^s_{loc}(p)$, $W^u_{loc}(p)$, of the same dimensions as those of the eigenspaces E^s, E^u of the linearized system (24), and tangent to E^s, E^u at p; see Figure 5.

Proof: Guckenheimer-Holmes [Ref. 4] references the proof, which uses the Implicit Function Theorem from advanced calculus.

An example which uses the result of Theorem 2 is the nonlinear system

$$\begin{aligned} x_1' &= x_1 \\ x_2' &= x_1^2 - x_2 \end{aligned} \tag{28}$$

which has a unique equilibrium point at the origin (0,0). The associated linear system about the point (0,0) is

$$x' = \begin{bmatrix} 1 & 0 \\ 0 & -1 \end{bmatrix} x \; . \tag{29}$$

$Df(0,0)$ has eigenvalues 1 and -1 with associated eigenvectors [1, 0] and [0, 1], respectively.

Thus by Theorem 2, the nonlinear system about the point (0,0) has a one-dimensional unstable manifold $W^u_{loc}(0,0)$ tangent to [1, 0], and a one-dimensional stable manifold $W^s_{loc}(0,0)$ tangent to [0, 1]. This can be verified by direct computation. First, if $x_1(0) = 0$ (i.e., an initial point is chosen on the x_2-axis), then it follows by solving the first equation of (28) that $x_1(t) \equiv 0$ for all $t \geq 0$, and thus by the second equation of (28), $x_2(t) \to 0$ as $t \to = +\infty$. Hence $W^s_{loc}(0) = E^s(0)$. Moreover, the explicit solution to (28) can be represented (non-parametrically) by the curves $x_2 = \frac{1}{3}x_1^{\,2} + Cx_1^{\,-1}$; then $W^u_{loc}(0)$ is the

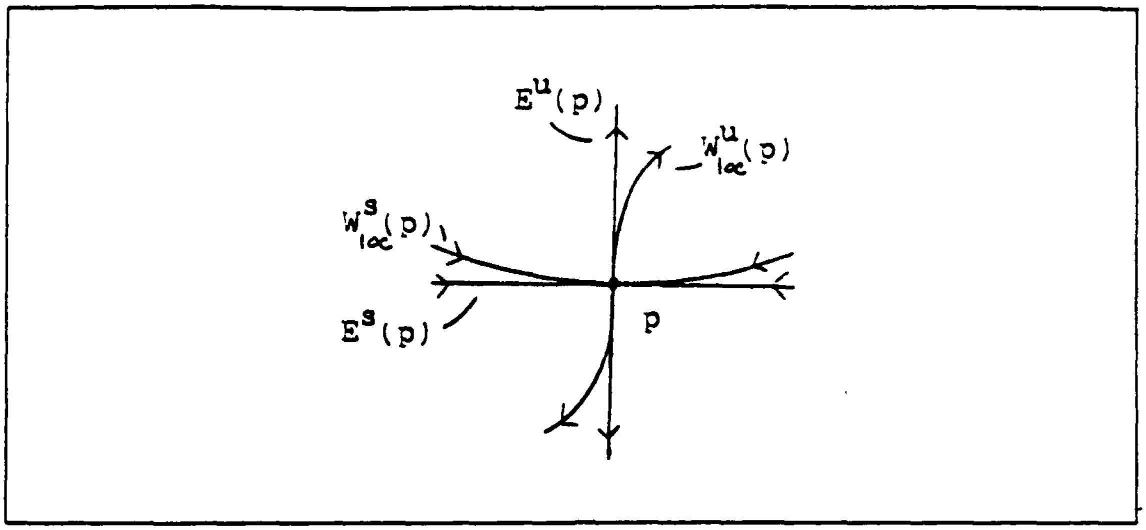

Figure 5. Schematic for Theorem 2

parabolic member of this family corresponding to $C = 0$. Figure 6 depicts the eigenspaces and manifolds for this example.

The local manifolds $W^s_{loc}(p)$, $W^u_{loc}(p)$ have global analogues independent of the U in (26) and (27) which are defined by letting $t \to -\infty$ and $t \to +\infty$, respectively:

$$W^s(p) = \bigcup_{t \leq 0} \phi_t(W^s_{loc}(p)) \tag{30}$$

$$W^u(p) = \bigcup_{t \geq 0} \phi_t(W^u_{loc}(p)) \ . \tag{31}$$

If $Df(p)$ has eigenvalues with real part equal to zero, then there also exists a corresponding **center manifold** $W^c(p)$, tangent to, and having the same dimension γ as, the center eigenspace E^c. The existence of $W^c(p)$, which need *not* be unique for a given system, is the content of the **Center Manifold Theorem.** The dynamics of a system on this manifold are generally more complicated than on the others, and a detailed analysis is beyond the scope of this thesis. Guckenheimer-Holmes [Ref. 4] provide a detailed discussion of center manifolds.

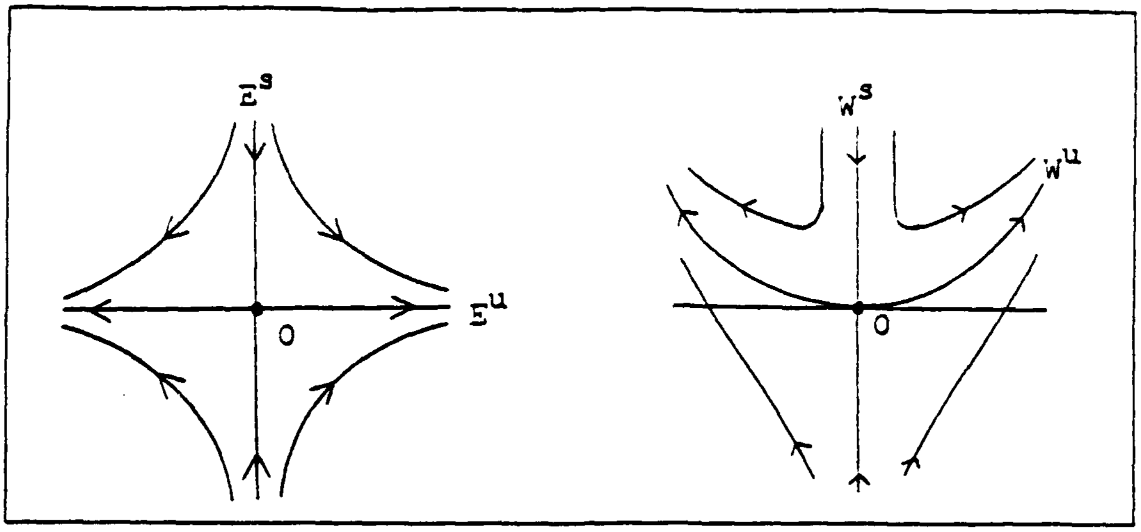

Figure 6. Eigenspaces and Manifolds

Clearly, by definition, $W^s(p)$ and $W^u(p)$ are invariant under the flow $\phi_t(x)$, and $p \in W^s(p) \cap W^u(p)$. If there exists a distinct point $q \in W^s(p) \cap W^u(p)$ as well, then it follows that $\phi_t(q) \rightarrow p$ as $t \rightarrow \pm\infty$, and q is said to be a **homoclinic point** to p, with corresponding **homoclinic orbit** $\phi_t(q)$, $-\infty < t < \infty$. Clearly, if q is homoclinic to p, then so is any other point in the orbit $\phi_t(q)$, hence there will be an infinite number of such points in general. Figure 7 illustrates a homoclinic orbit.

The formation of homoclinic points and orbits plays an important role in the development of chaotic dynamical behavior, as will be observed in subsequent chapters.

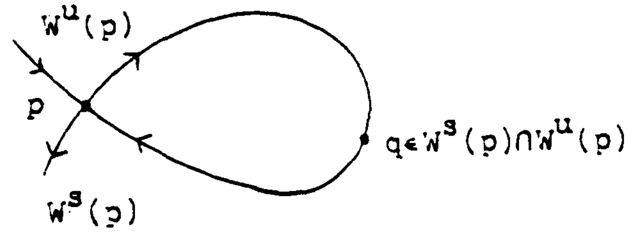

Figure 7. Homoclinic orbit

III. DEFINING CHAOS

A. POINCARÉ MAPS

As we shall see, there are many ways to approach the definition of "chaos." We begin with one such approach, Poincaré maps. As seen earlier, one way to help characterize the dynamic behavior of a nonlinear system of differential equations is to linearize it in a local area. Another technique is to discretize it. By analyzing "snapshots" of a continuous solution, we can infer certain properties about it. These "snapshots" (discretization) form the foundation for Poincaré maps.

We start with a third order ($x \in \mathbb{R}^3$) autonomous system and a suitable two-dimensional surface (for example, a plane) Π such that the flow $\phi_t(x)$ under observation repeatedly intersects Π transversely (i.e., nontangentially). The image of a point $x \in \Pi$ under the **first return** or **Poincaré map** $P: \Pi \rightarrow \Pi$ is defined as that point along the flow $\phi_t(x)$ which next intersects the surface Π . Varying definitions are possible if the direction in which $\phi_t(x)$ crosses Π is taken into account. There are also cases where a well-defined Poincaré map is not possible. Moreover the definition of a Poincaré map can be extended to the general case $x \in \mathbb{R}^n$, n > 3. Instead of using a two-dimensional surface for Π , a hypersurface of dimension (n-1) is chosen. Figure 8 shows the construction of a Poincaré map for $x \in \mathbb{R}^3$.

As with continuous systems, discrete systems have their own accompanying set of definitions and properties. A common example of a discrete dynamical system is an iterated function. Although the following definitions are stated for one dimension we will show how they can be extended to higher dimensions.

Given a function $g: \mathbb{R} \rightarrow \mathbb{R}$ and an initial value $x_0 \in \mathbb{R}$, the sequence $\{x_0, g(x_0), g(g(x_0)), g(g(g(x_0))), ...\}$ is defined as the ***forward orbit*** of x_0 under g . Note that

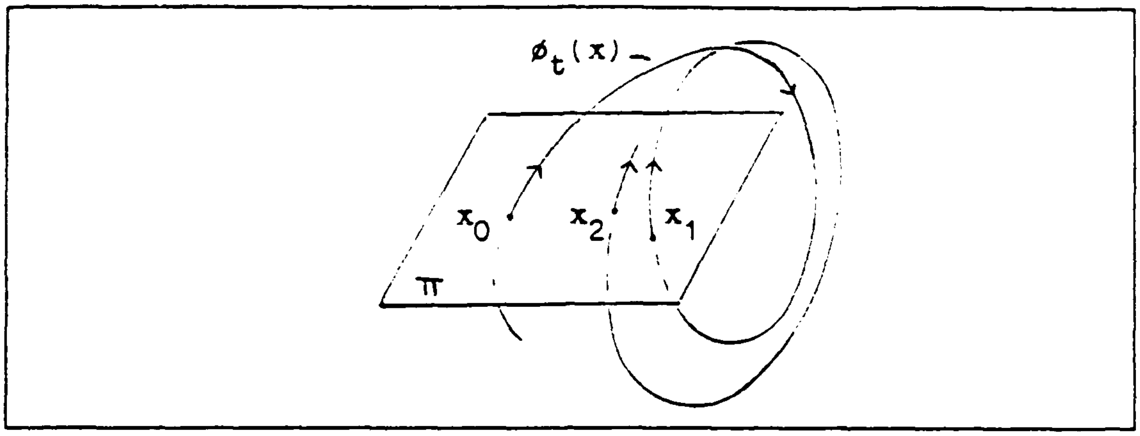

Figure 8. Poincaré Map

the recursive formula $x_{n+1} = g(x_n)$ with initial condition x_0 is an equivalent definition for the forward orbit. Provided that g has an inverse, the **backward orbit** of x_0 under g is defined as $\{x_0, g^{-1}(x_0), g^{-1}(g^{-1}(x_0)), \ldots\}$. (This definition can be generalized by using $g^{-1}(x) = \{y \in \mathbb{R}: g(y) = x\}$.) The **full orbit** of x_0 under g is defined as $\{\ldots, g^{-1}(g^{-1}(x_0)), g^{-1}(x_0), x_0, g(x_0), g(g(x_0)), \ldots\}$. Forward and backward orbits of g are comparable to the forward and backward orbits of a flow $\phi_t(x)$ in the continuous system. Thus, the sequence of points $\{x_0, x_1, x_2, \ldots\}$ generated by the intersection of the flow $\phi_t(x)$ with Π in Figure 8 is the forward orbit of a point x_0 under the Poincaré map $P: \Pi \rightarrow \Pi$.

In discussing iterative functions it is convenient to use the following notation:

$$g^n(x) = \underbrace{(g \circ g \circ \ldots \circ g)}_{\text{n times}}(x), \tag{32}$$

for n = 1,2,3,..., where the symbol o denotes function composition, and $g^{-n}(x) = (g^{-1}(x))^n$. The point p is defined as a **fixed point** of g if $g(p) = p$. A point q which is not a fixed point is defined as **eventually fixed** if $g^m(q)$ is fixed for some $m \in \mathbb{Z}^+$. More generally, a point p is **periodic** of **period n** if $g^n(p) = p$. Note that if p has period n, then it automatically has periods of all (positive) integer multiples of n. This motivates the next definition: a point p is **periodic** of **prime period n** if $g^n(p) = p$ and there does not exist an m such that $0 < m < n$ and $g^m(p) = p$. A point q which is not periodic is defined as **eventually periodic** if $g^m(q)$ is periodic for some $m \in \mathbb{Z}^+$.

The definitions above extend to spaces other than $\mathbb{R}$. For example, consider **code space** Σ, the collection of all infinite binary strings $s_1s_2s_3\ldots$, $s_i \in \{0,1\}$, and the **shift map** $g: \Sigma \rightarrow \Sigma$ given by

$$g(s_1 s_2 s_3 \ldots) = s_2 s_3 s_4 \ldots \quad . \tag{33}$$

The fixed points of g are $0\overline{00}$, $1\overline{11}$ (The bar indicates an infinite repeating block). The point $010\overline{00}$ is eventually fixed. The point $001\overline{001}$ is a periodic point of prime period three. The point $10001\overline{001}$ is eventually periodic.

Given that g is differentiable the following definitions also hold. A periodic point of prime period n is **hyperbolic** if $|(g^n)'(p)| \neq 1$. Note that a fixed point is equivalent to a periodic point of prime period one. Thus a fixed point is hyperbolic if $|g'(p)| \neq 1$. Also note that $(g^n)'(p)$ in general is calculated by the Chain Rule:

$$(g^n)'(p) = g'(g^{n-1}(p)) \cdots g'(g(p))g'(p) \,. \tag{34}$$

For example, if p is a periodic point of prime period three of the sequence $\{p = 1, \;\; g(p) = 0, \;\; g^2(p) = -1, \;\; g^3(p) = 1, \ldots\}$ then

$$(g^3)'(1) = g'(-1)g'(0)g'(1) \;. \tag{35}$$

Clearly, this is also the common value of $(g^3)'(0)$ and $(g^3)'(-1)$. A periodic point p is **non-hyperbolic** if $|(g^n)'(p)| = 1$. A periodic point p of prime period n is **attracting** if $|(g^n)'(p)| < 1$. The point p is **repelling** if $|(g^n)'(p)| > 1$. A good introductory reference that covers chaos for discrete systems is Beaver [Ref. 1]. A more rigorous treatment is found in Devaney [Ref. 6].

For higher dimensions $\mathbb{R}^m$ the iterative system takes the form

$$\begin{bmatrix} x_{n+1}^{(1)} \\ x_{n+1}^{(2)} \\ \cdot \\ \cdot \\ x_{n+1}^{(m)} \end{bmatrix} = \begin{bmatrix} g^{(1)}(x_n^{(1)}, x_n^{(2)}, \ldots, x_n^{(m)}) \\ g^{(2)}(x_n^{(1)}, x_n^{(2)}, \ldots, x_n^{(m)}) \\ \cdot \\ \cdot \\ g^{(m)}(x_n^{(1)}, x_n^{(2)}, \ldots, x_n^{(m)}) \end{bmatrix}, \tag{36}$$

equivalently,

$$x_{n+1} = g(x_n) \tag{37}$$

where $x \in \mathbb{R}^m$ and $g\colon \mathbb{R}^m \to \mathbb{R}^m$.

Definitions for higher dimensions extend in the obvious manner with the exception of the hyperbolic, attracting and repelling periodic points. A periodic point p of prime period n is **hyperbolic** if the Jacobian matrix $D(g^n)(p)$ has no eigenvalues of unit modulus, that is, no eigenvalues on the unit circle $|z| = 1$ in the complex plane. (We remark that this definition extends to all points of any limit set Λ; in this case we say that the entire set Λ is hyperbolic.) The Jacobian can be computed with the aid of the Chain Rule as before:

$$D(g^n)(p) = Dg(g^{n-1}(p)) \ldots Dg(g(p))Dg(p). \tag{38}$$

The multiplications above are matrix multiplications. If all the eigenvalues of $D(g^n)(p)$ have modulus less than one then the periodic point p is **attracting.** If all the eigenvalues have modulus greater than one, p is **repelling.** An attracting fixed point can be shown to be asymptotically stable, and hence is sometimes referred to as a **sink.** Likewise a repelling fixed point is said to be a **source.** If some eigenvalues lie in the interior of the unit disk while the remaining ones lie outside, then a fixed point p is a **saddle point.**

As one might expect, eigenspaces and manifolds exist for discrete systems similar to those just discussed in the previous section for continuous systems. The position of the eigenvalues in relation to the complex unit circle is the determining factor for discrete systems, as opposed to continuous systems where it is their position relative to the imaginary axis (i.e., stable if $\mathrm{Re}\{\lambda\} < 0$, unstable if $\mathrm{Re}\{\lambda\} > 0$, etc.). The interested reader is referred to Guckenheimer-Holmes [Ref. 4].

We now return to the process of using the information gained by Poincaré maps to characterize the behavior of an n^{th} order nonlinear continuous system. Recall that in this case, the Poincaré map is a mapping between two (n-1)-dimensional spaces.

By construction, a periodic orbit of a continuous system corresponds to a discrete periodic cycle of some Poincaré map (Figure 9), such as a fixed point, for example. If the fixed point is stable then the periodic orbit is asymptotically stable. If the fixed point is unstable then so is the periodic orbit. If the fixed point is neither stable nor unstable it is possible to relate the dimensions of the manifolds of the fixed point to the manifolds of the periodic orbit. The reader is referred to Guckenheimer-Holmes [Ref. 4] for a more in-depth discussion of the relation between the discrete manifolds of the Poincaré map and the manifolds of the continuous system.

A quasi-periodic orbit of a continuous system that consists of only two incommensurate periods corresponds to some Poincaré map of embedded circles. For a quasi-periodic orbit of K incommensurate periods the Poincaré map consists of a generalized (K-1) - tori. The idea is that for a quasi-periodic orbit the corresponding Poincaré map is one of compact (closed, bounded) geometric structure. For a discussion of Poincaré maps corresponding to quasi-periodic orbits see Parker-Chua [Ref. 7].

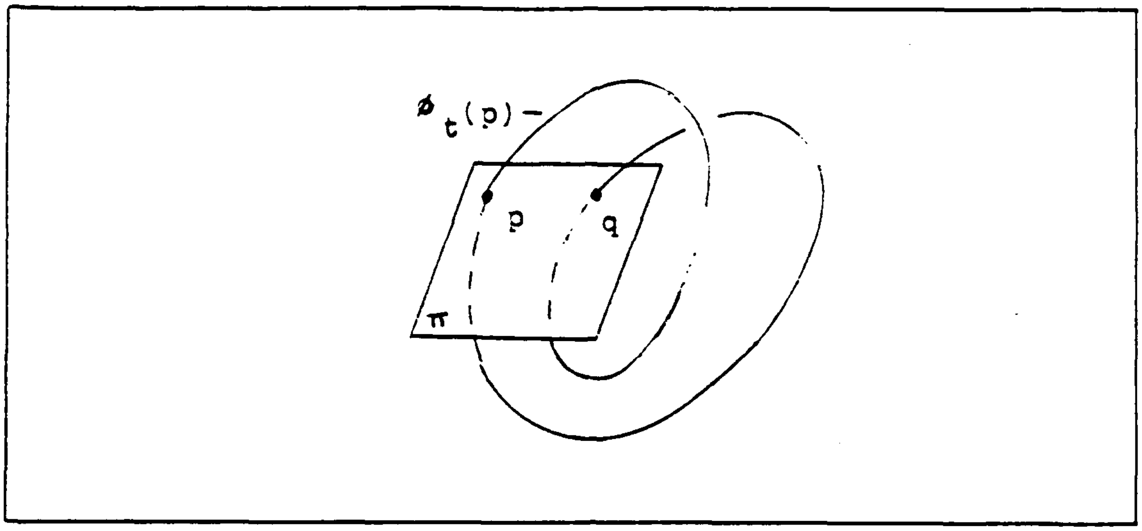

Figure 9. Poincaré Map for a Periodic Orbit

Although we have yet to define chaos, those continuous orbits which are chaotic have corresponding Poincaré maps whose images are very distinctive and often quite beautiful. These images are distinctive in that they seem to possess a more complex geometric structure than those of periodic or quasi-periodic orbits. In an effort to quantify this apparent increased complexity, various definitions of "dimension" have been formulated which for these exotic sets can take on *non-integer* values. Several of these definitions are discussed in a subsequent chapter.

B. SMALE HORSESHOE

We continue our approach toward a definition of chaos with the following example of the Smale Horseshoe map, a two-dimensional discrete map that exhibits many of the features which are normally associated with "chaotic" dynamical systems. This map can arise as a Poincaré map for a three-dimensional autonomous system. It is also closely related to homoclinic orbits which were briefly introduced at the end of the section on manifolds.

Before beginning our example a few preliminaries are needed. We have already seen how the ability to relate the dynamics of one system to another can be very powerful. Another much stronger method for accomplishing this relation is topological conjugacy.

Let S and T be sets; the function h: S $\rightarrow$ T is a **homeomorphism** if it is continuous, one-to-one, onto and has a continuous inverse. Two maps f: S $\rightarrow$ S and g: T $\rightarrow$ T are said to be **topologically conjugate** if there exists a homeomorphism h: S $\rightarrow$ T such that $h \circ f = g \circ h$. The function h is defined as the **topological conjugacy.** Figure 10 is a schematic for topologically conjugate maps f and g, and we say that the diagram "commutes."

The following is an example of two topologically conjugate functions. Let S = [0,1], T = [$-\frac{1}{2}$, $\frac{1}{2}$], and let f: S $\rightarrow$ S, g: T $\rightarrow$ T, and h: S $\rightarrow$ T be given by

$$
\begin{aligned}
f(x) &= x(1 - x) \\
g(x) &= x^2 + .25 \\
h(x) &= -x + .5 \ .
\end{aligned}
\tag{39}
$$

Then

$$
\begin{aligned}
& h \circ f = x^2 - x + .5 \\
\text{and} \quad & g \circ h = x^2 - x + .5 \ .
\end{aligned}
\tag{40}
$$

Since $h \circ g = g \circ h$ and h is a homeomorphism, the functions f, g are topologically conjugate.

The power of this relation is that topologically conjugate maps f and g have completely equivalent dynamics. If f has a stable fixed point p then g has a stable fixed point $h(p)$. More generally, any given orbit of f is mapped to a corresponding orbit with equivalent dynamics in g via the homeomorphism h. For the example above, $p = 0$ is a non-hyperbolic fixed point for f and $h(0) = 0.5$ is a non-hyperbolic fixed point for g;

$$
\begin{tikzcd}
S \arrow[r, "f"] \arrow[d, "h"'] & S \arrow[d, "h"] \\
T \arrow[r, "g"] & T
\end{tikzcd}
$$

Figure 10. Topological Conjugacy

equivalent dynamics are in fact suggested by comparing the graphs of f and g, respectively.

Thus if we are able to establish a topological conjugacy between a map with unknown dynamics and one with which we are well acquainted, then the dynamics of the original map will be completely known. As expected, it may not be an easy task to establish such a topological conjugacy.

The other concept we will need in discussing the Smale Horseshoe is one we have already covered for continuous systems. An **invariant set** Λ for a general map $f: S \to S$ is a subset $\Lambda \subseteq S$ such that $f(\Lambda) = \Lambda$, where $f(\Lambda) = \{f(x): x \in \Lambda\}$. Fixed points and periodic sequences are trivial examples of invariant sets. A method of constructing an invariant set for f, which may not be trivial, is to take the infinite intersection of the forward iterates of the entire domain and intersect them with the corresponding backward iterates, that is,

$$
\begin{aligned}
\Lambda &= \bigcap_{n=-\infty}^{\infty} f^n(S) \\
&= \lim_{m \to \infty} \bigcap_{n=-m}^{m} f^n(S) .
\end{aligned}
\tag{41}
$$

It is this construction which we will use to obtain an invariant set for the Smale Horseshoe map.

Let S be the unit square I^2; contract it vertically by a factor of one-quarter, and expand it horizontally by a factor of four. Next bend it into a horseshoe-like shape and superimpose it back onto the unit square S. Call this geometric mapping f. The map $f: S \rightarrow S$ can be formulated algebraically but the geometric presentation promotes clarity, and is diagrammed in Figure 11.

Let m = 1 in (41); the first iteration $f(S)$ consists of two horizontal bars which we have labeled H^0 and H^1. In order to find the backward iterates, perform the map in reverse. This process is shown in Figure 12, and results in two vertical bars, labeled V^0 and V^1, respectively, such that $f(V^0) = H^0$ and $f(V^1) = H^1$. The intersection of one forward iteration and its backward iteration is shown in Figure 13, and results in four shaded blocks which contain the invariant set Λ. Each block can therefore be represented as some $H^{s_{-1}} \cap V^{s_0}$, where $s_{-1}, s_0 \in \{0,1\}$, which then corresponds to a unique binary address of the form $s_{-1}.s_0$, also shown in Figure 13. Thus, any point x in such a block has the property that $x \in V^{s_0}$ and $x \in H^{s_{-1}}$, the latter of which implies that $f^{-1}(x) \in V^{s_{-1}}$. This suggests that the vertical bars V^0 and V^1 may eventually be used as the basis for tracking the orbit of a point in Λ via a binary sequence.

Let m = 2 in (41); we now consider the forward and backward iterations of the intersection depicted in Figure 13. These second forward and backward iterations are shown in Figures 14 and 15. Notice that the second forward iteration gives rise to four horizontal bars which are subsets of H^0 and H^1. (Equivalently, these four horizontal bars can also be characterized as $f^2(S)$; see Figure 16.) The second backward iteration results in four vertical bars. Like the horizontal bars, the four vertical bars are subsets of V^0 and V^1. The intersection results in sixteen blocks (see Figure 17) which contain Λ, and may be assigned four-digit binary addresses according to a prescription similar to that given above.

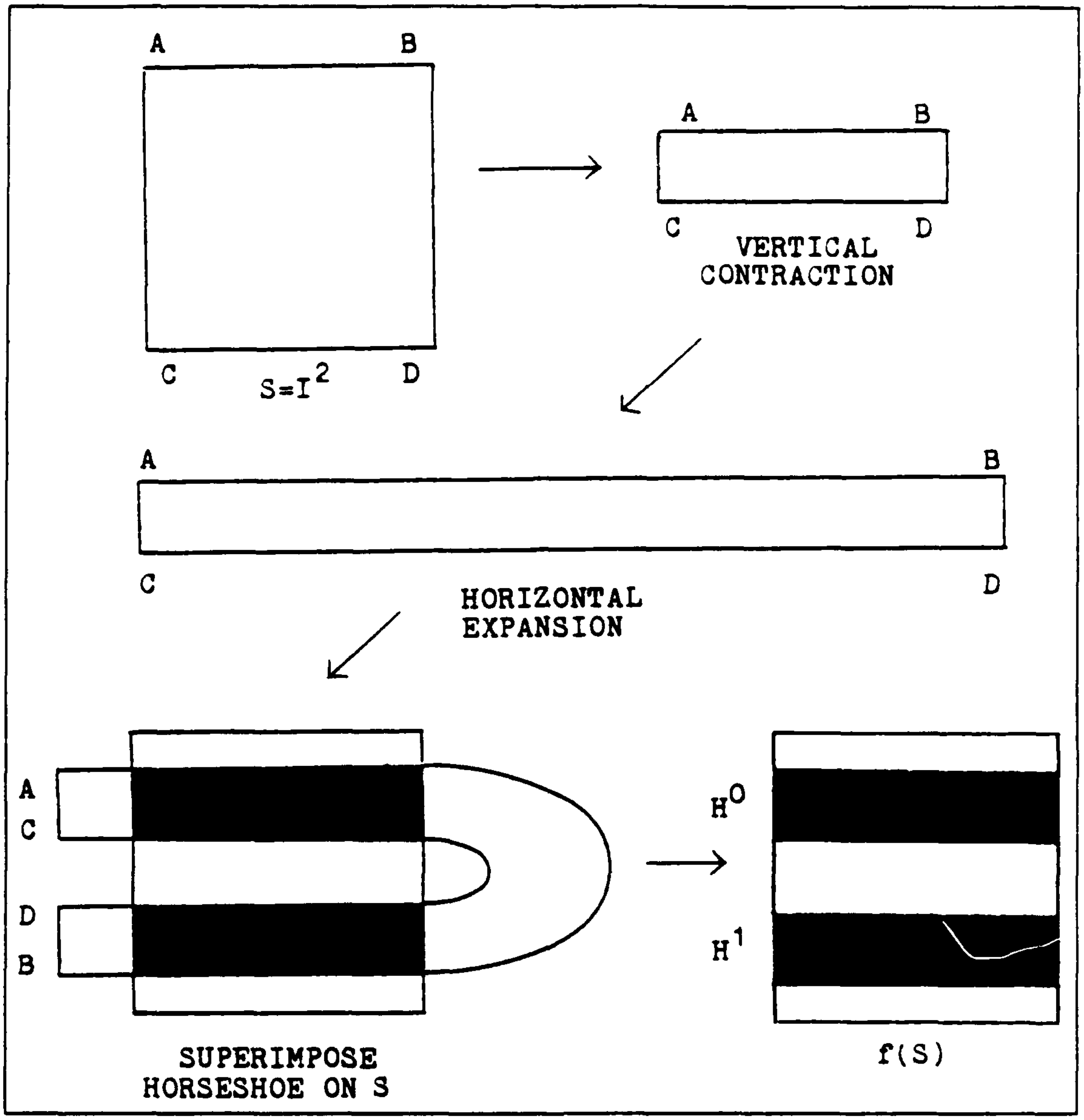

Figure 11. First Forward Iteration

In general, the n^{th} forward iteration will result in 2^n horizontal bars which are subsets of the 2^{n-1} horizontal bars of $(n-1)^{th}$ forward iteration, and likewise for the vertical bars with respect to backward iteration. By taking the *infinite* intersection of the forward iterates of S and intersecting them with their corresponding backward iterates, we con-

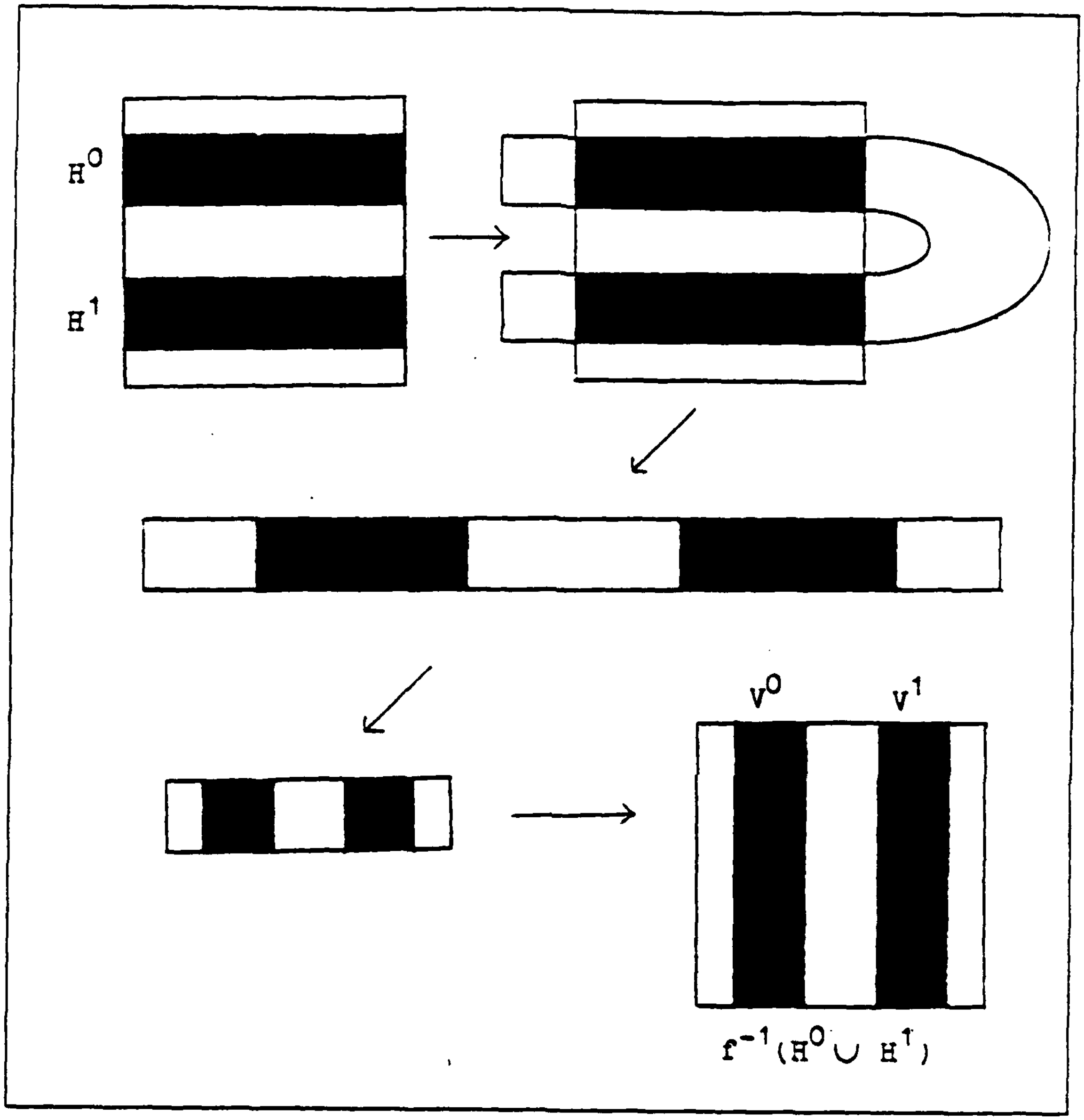

Figure 12. First Backward Iteration

struct (by the Heine-Borel Theorem of advanced calculus) a nonempty invariant set Λ of f, and a map h on Λ such that each and every point $x \in \Lambda$ has a corresponding address, or **itinerary**, $h(x)$, which is representable by a binary bi-infinite sequence:

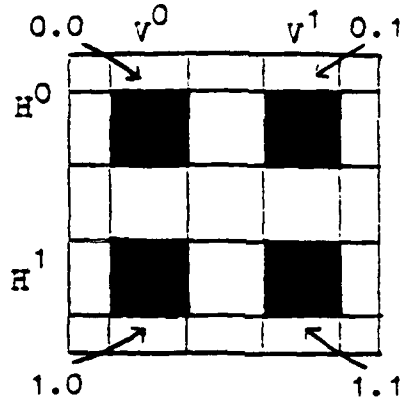

Figure 13. First Iteration Intersection

$$h(x) = \ldots s_{-3}s_{-2}s_{-1}.s_0s_1s_2\ldots, \tag{42}$$

where

$$s_i = \begin{cases} 0, & f^i(x) \in V^0 \\ 1, & f^i(x) \in V^1 \end{cases}. \tag{43}$$

This sequence is similar to the code space used in (33) except that it is bi-infinite. We will denote this space of binary bi-infinite sequences as Σ'. It is possible to show that the map $h: \Lambda \rightarrow \Sigma'$ is a homeomorphism, and is an example of the use of **symbolic dynamics.**

Finally we define a shift map $g: \Sigma' \rightarrow \Sigma'$ such that

$$g(\ldots s_{-3}s_{-2}s_{-1}.s_0s_1s_2\ldots) = \ldots s_{-2}s_{-1}s_0.s_1s_2s_3\ldots \ . \tag{44}$$

Theorem 3: The maps f and g defined above are topologically conjugate with topological conjugacy h .

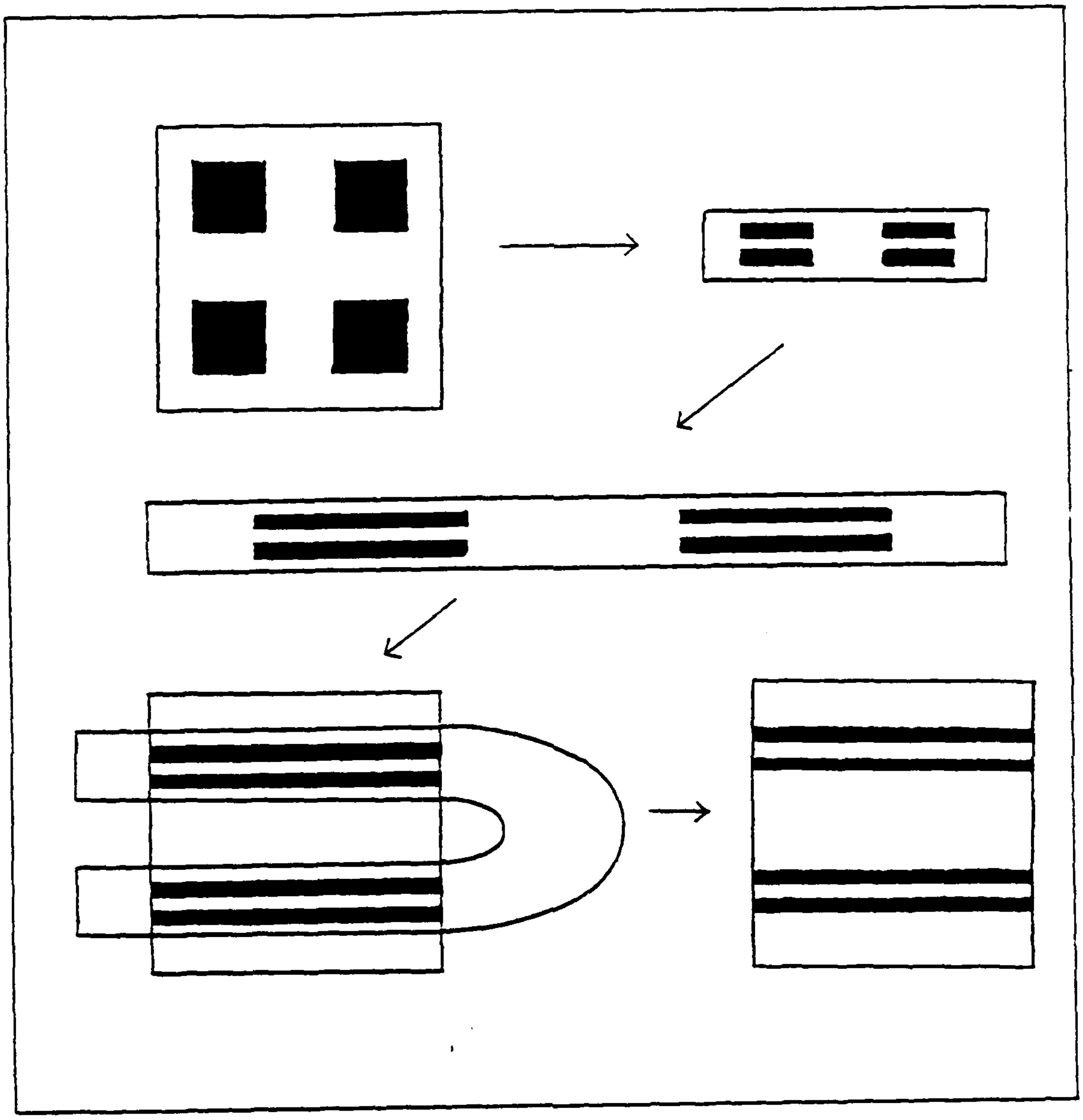

Figure 14. Second Forward Iteration

Proof: The proof of this theorem is closely linked to the proof of Theorem 5.1.1 of Guckenheimer-Holmes [Ref. 4].

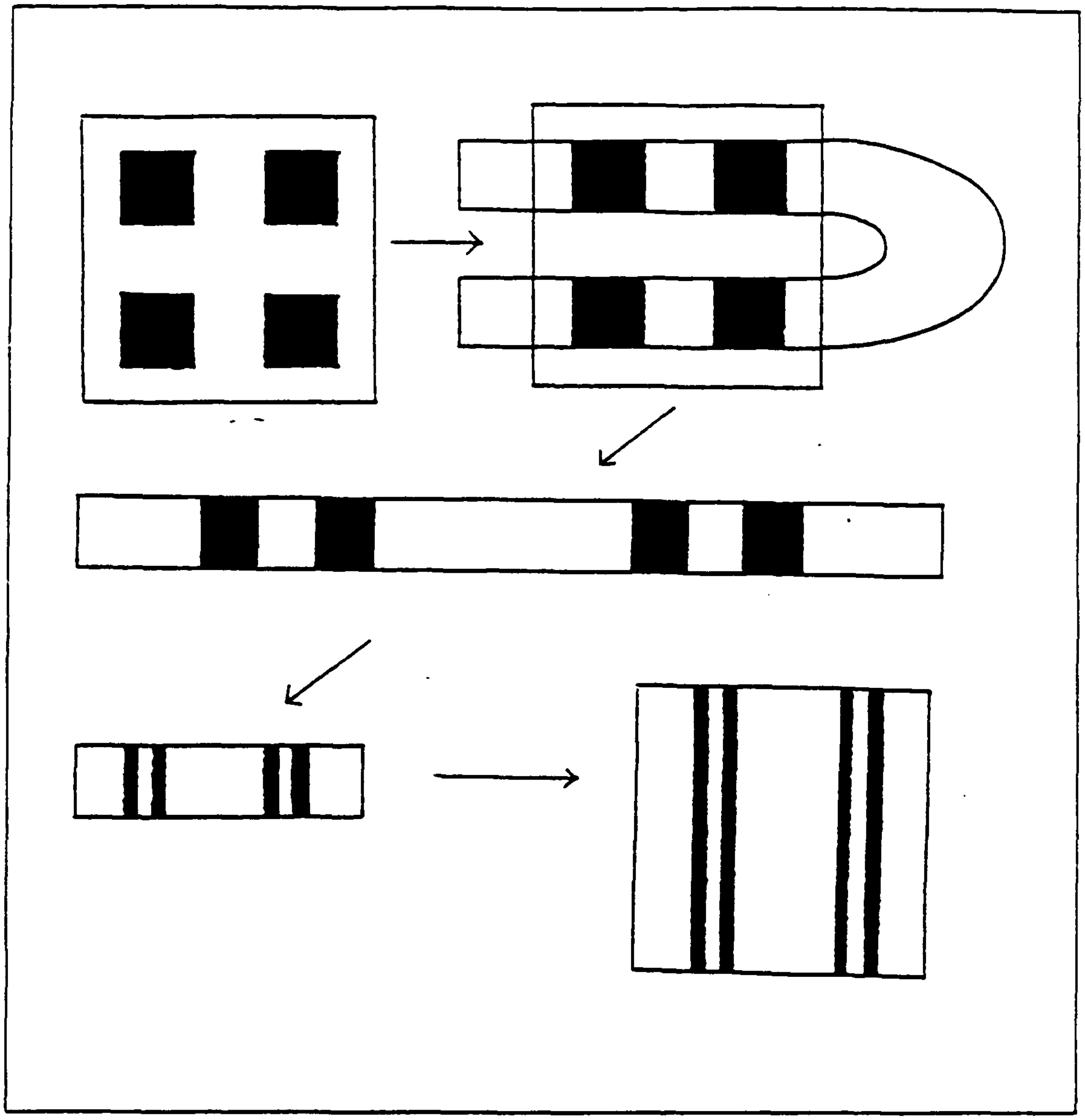

Figure 15. Second Backward Iteration

Since f and g are topologically conjugate we can equate the dynamic behavior of g with that of f. The map g has certain properties which will form the definition for chaos in the next section.

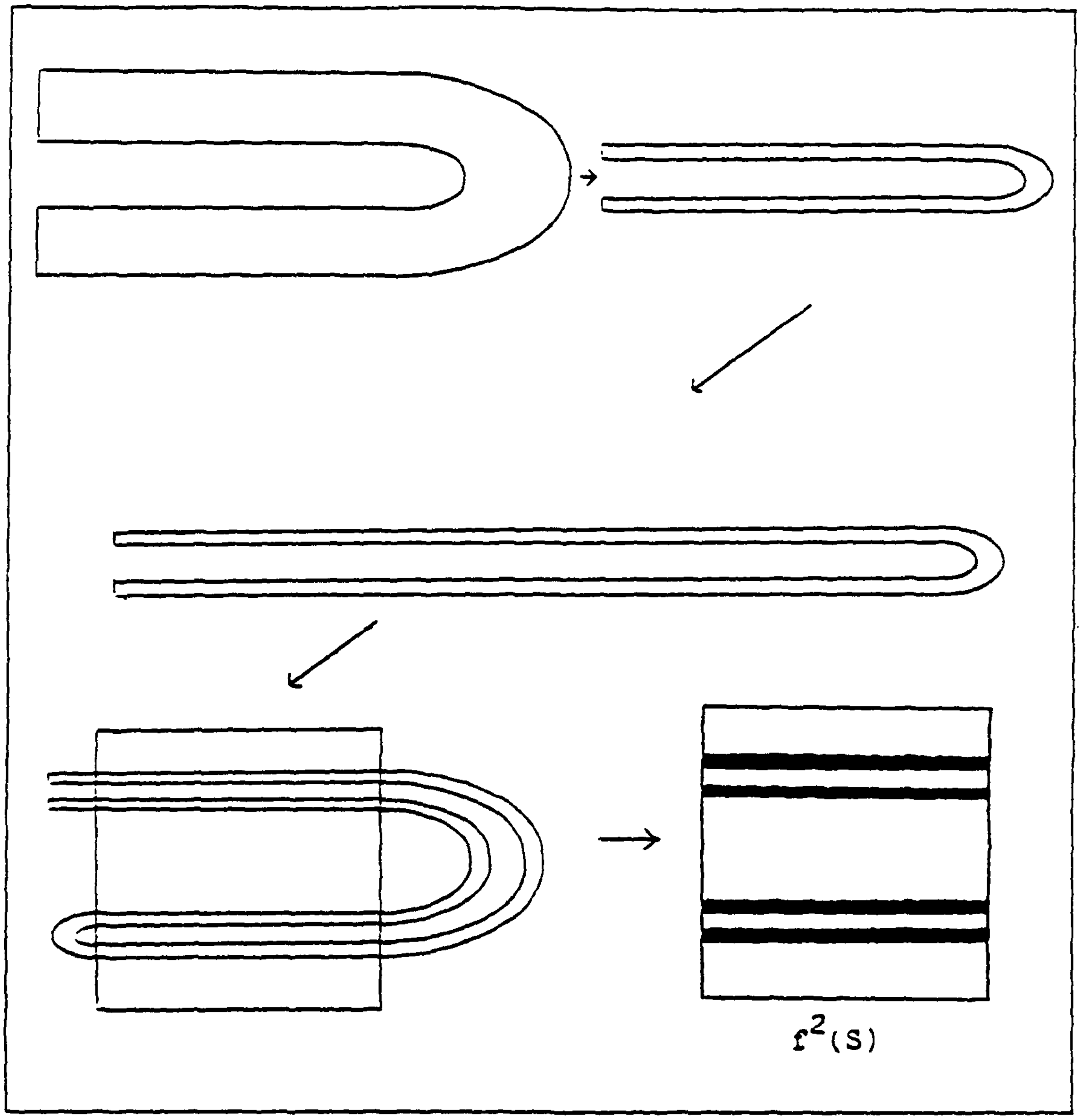

Figure 16. f^2(S)

Our first goal is to show that two points in Σ', initially "close", start to diverge from one another under forward iterations of g. This property of a map is known as sensitive dependence on initial conditions. A mathematical definition is given by Devaney [Ref. 6]. A map $g: T \rightarrow T$ has **sensitive dependence on initial conditions** on T if there

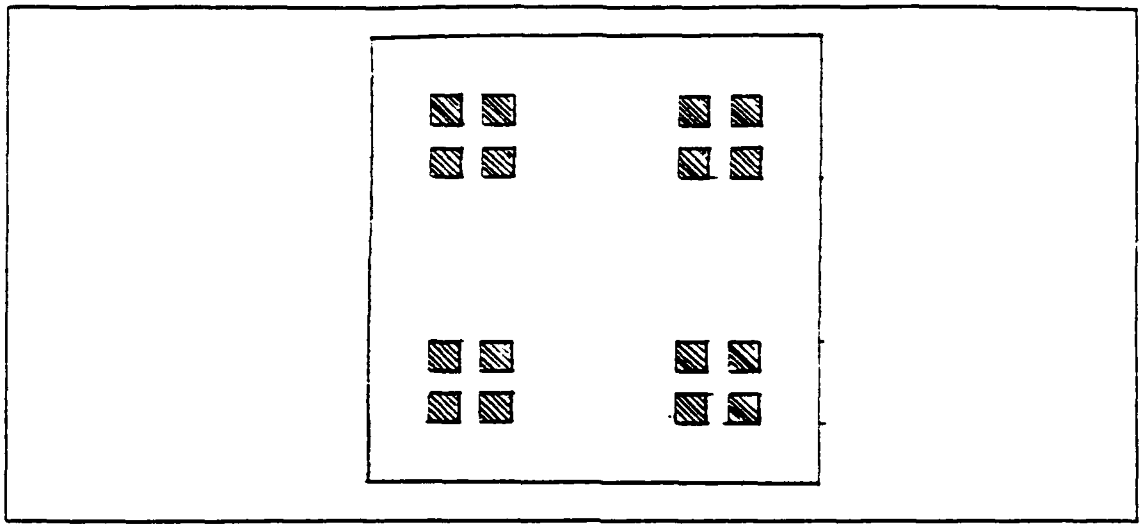

Figure 17. Second Iteration Intersection

exists $\varepsilon > 0$ such that, for any $x \in$ T and any δ-neighborhood N of x, there exists $y \in$ N and n ≥ 0 such that $d(g^n(x), g^n(y)) > \varepsilon$.

In the previous definition $d(s, t)$ represents an appropriate "distance measuring" function, or **metric** for the space T. For our example the space T is equal to Σ' and

$$d(s, t) = \sum_{i=-\infty}^{\infty} \frac{|s_i - t_i|}{2^{|i|}} \tag{45}$$

for $s = \ldots s_{-1}.s_0s_1\ldots$ and $t = \ldots t_{-1}.t_0t_1\ldots$ in Σ'. Using the definition of sensitive dependence on initial conditions it is possible to show that the map g, and thus f, has this property with respect to the metric given above.

For example, suppose s and t agree in positions i = -100 to 100 and disagree in the remaining positions. Then s and t are initially "close" to one another: $d(s,t) < 2^{-99}$. However after 201 iterations of g, $g^{201}(s)$ and $g^{201}(t)$ are quite widely separated:

$d(g^{201}(s), g^{201}(t)) > 2.99$. In this way, given any arbitrarily small neighborhood N of s we can find a distinct point t in N such that $d(g^{n}(s), g^{n}(t)) > 2.99$ for some $n \geq 0$. Since f and g are topologically conjugate there are exactly two points x and y in Λ that correspond via the homeomorphism $h: \Lambda \rightarrow \Sigma'$ to the sequences s and t in Σ'. Hence f exhibits sensitive dependence on initial conditions on Λ .

Our second goal is to show that g is topologically transitive. Devaney [Ref. 6] defines a map $g: T \rightarrow T$ as **topologically transitive** on T if for any pair of open sets $U, V \subset T$ there exists $k > 0$ such that $g^{k}(U) \cap V \neq 0$, that is, any two subsets of T eventually intersect. If g contains a **dense orbit**, that is, if there exists a point s in Σ' whose orbit becomes arbitrarily close to all points in Σ', then it follows that g is topologically transitive.

Consider the point $\hat{s}$ constructed in the following manner:

$$\hat{s} = \ldots 0.\underbrace{0\,0\,01\;10\;11}_{\text{all 2-blocks}}\;\underbrace{0000\;0001\;\ldots\;1111}_{\text{all 4-blocks}}\;\underbrace{000000\;000001\;\ldots}_{\text{all 6-blocks}}\;\ldots \tag{46}$$

During the first seven iterations, the orbit of $\hat{s}$ will have agreed in the $i = -1$ and $i = 0$ positions with every point in Σ'. There are only four possible binary numbers of length two and in seven iterations the orbit of $\hat{s}$ has covered them.

In the next 64 ($2^4 \times 4$) iterations the orbit of $\hat{s}$ will have agreed in positions $i = -2$ to 1 with every point in Σ'. The construction of $\hat{s}$ is such that in a finite - although possibly large - number of iterations, the orbit of $\hat{s}$ will agree in positions $i = -n$ to $n-1$ with every point in Σ', for any $n \geq 0$. In other words, the orbit of $\hat{s}$ gets arbitrarily close to every number in Σ'.

Our final goal is to show that periodic points are dense in Σ' (i.e., show that every point in Σ' has a periodic point arbitrarily close to it). Consider any point $s \in \Sigma'$, then s can be represented as

$$s = \ldots s_{-n-1} s_{-n} s_{-n+1} \ldots s_{-1} . s_0 s_1 \ldots s_{n-1} s_n s_{n+1} \ldots \; . \tag{47}$$

Choosing an arbitrary distance between s and a periodic point $p \in \Sigma'$ is equivalent to choosing an n sufficiently large that p and s agree in positions i = -n to n. Thus construct p in the following manner:

$$p = \underline{s_0 s_1 \ldots s_{n-1} s_n s_{-n} s_{-n+1} s_{-1}} . \overline{s_0 s_1 \ldots s_{n-1} s_n s_{-n} s_{-n+1} \ldots s_{-1}} \; . \tag{48}$$

The bar underneath indicates repeated blocks to the left and the bar on top indicates repeated blocks to the right. Note that p agrees with s in positions i = -n to n and is periodic of order 2n + 1. By constructing p in this manner we have shown that any $s \in \Sigma'$ has a periodic point arbitrarily close to it. Therefore periodic points of g are dense in Σ'.

In summary, $g: \Sigma' \rightarrow \Sigma'$ is a map for which

1. g has sensitive dependence on initial conditions,
2. g is topologically transitive,
3. periodic points of g are dense in Σ'.

Since g is topologically conjugate to the Smale Horseshoe map $f: \Lambda \rightarrow \Lambda$, f and g share these three properties.

There is in addition an intimate connection between this map and the existence of homoclinic points, which we will state more precisely in the following chapter. Recall that a point q is homoclinic to a fixed point p if $q \neq p$ and $q \in W^s(p) \cap W^u(p)$. Now, since $f(V^0) = H^0$, it follows that the block $V^0 \cap H^0$ is mapped to itself by f, hence it contains a fixed point p having itinerary $\underline{0}.\overline{0}$. Clearly, any point q with itinerary $\underline{0} s_{-m} \ldots s_{-1} . s_0 \ldots s_n \overline{0}$ has the property that

$$d(g^k(p), g^k(q)) \rightarrow 0 \quad \text{as} \quad k \rightarrow \pm\infty \,, \tag{49}$$

thus $q \in W^s(p) \cap W^u(p)$, and there are infinitely many such intersection points q. Moreover, we may similarly construct a point q satisfying (49) for *any* point $p \in \Lambda$; in this case q is both **forward** and **backward asymptotic** to p, respectively.

The convoluted intertwining of the stable and unstable manifolds is a result of the shrinking, stretching, and folding effects of the map and leads to sensitive dependence on initial conditions, topological transitivity and dense periodic points (see Figure 18). For this reason, in practice, the numerical detection of horseshoes in a particular dynamical system is often identified with the presence of chaos.

It should be noted that the Smale Horseshoe map has many variations. Although our map contracted and expanded by orders of four they can be generalized to a contraction factor μ , $0 < \mu < ½$ and an expansion factor λ , $\lambda > 2$. The orientation of the horseshoe with respect to the unit square need not be horizontal or vertical. Even the unit square may be varied to other domains.

Note also that the use of symbolic dynamics enabled us to take what were only observations (geometric properties of the Smale Horseshoe map) and make them mathematically precise. That is, we were able to perform rigorous analysis which was not possible earlier without the use of symbolic dynamics.

The invariant limit set Λ also requires further discussion. It is constructed by an explicit procedure that results in a sequence of disconnected sets which have some interesting properties. Note that each of the small groups of four blocks in Figure 17 is a contracted and translated copy of Figure 13, as each block in Figure 13 is such a copy of the original unit square S in Figure 11. This property of **self-similarity** persists throughout the procedure and ultimately carries through to the invariant set Λ itself. This kind of recursive construction - sometimes referred to as an **iterated function system** (IFS) - can be used as the basis for computer generation of other types of "fractal" images. These limit sets may be viewed as "attractors" of certain "affine maps" (linear fol-

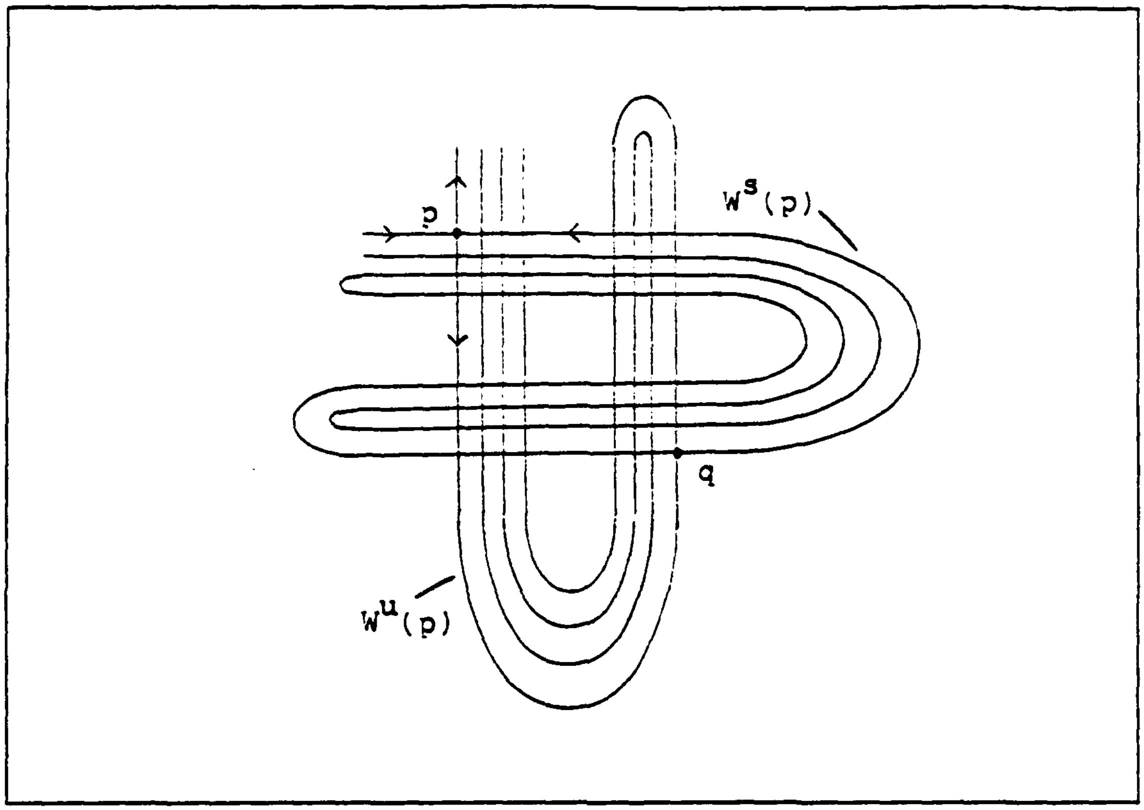

Figure 18. Intertwining of Stable and Unstable Manifolds

lowed by a translation, thus representable by matrices) on subsets of $\mathbf{R}^n$, and therefore can be addressed by using a variation of code space. The resulting fractal attractor Λ is unique, and has "dimension" which is not necessarily an integer, but may be a fractional value, for example (and hence the name). For a discussion of iterated function systems see Beaver [Ref. 1].

The invariant limit set Λ of the Smale Horseshoe is itself closely related to a well-known subset of the interval [0, 1], the Cantor Ternary or Middle-Thirds Set. This set is constructed recursively by the repeated removal of open middle thirds from all current intervals. Thus, removing the open middle third from [0, 1] results in two closed intervals: $[0, \frac{1}{3}]$ and $[\frac{2}{3}, 1]$. Repeating this procedure results in four closed intervals:

$[0, \frac{1}{9}]$, $[\frac{2}{9}, \frac{1}{3}]$, $[\frac{2}{3}, \frac{7}{9}]$ and $[\frac{8}{9}, 1]$. Upon infinite iteration we are left with the Cantor set. Although this straightforward construction may seem rather trivial, the Cantor set has many interesting properties which are shared by the invariant set Λ. For example, both the Cantor set and the set Λ are **totally disconnected,** that is, for every $x \in \Lambda$ there exists an open ball, $B_\delta(x) = \{y: d(x,y) < \delta\}$ centered at x of radius δ which contains no points of Λ other than x. In fact, Λ itself may be viewed as a "higher dimensional" version of the classical Cantor set that exists in the unit square rather than the unit interval. For a more complete discussion of fractals and the Cantor set see Beaver [Ref. 1].

C. CHAOS

There is no universally accepted definition for chaos. For discrete systems we shall adopt the definition given by Devaney [Ref. 6]. Let S be a set. The map f: S → S is said to be **chaotic on S** if

1. f has sensitive dependence on initial conditions,
2. f is topologically transitive,
3. periodic points of f are dense in S.

Note that the Smale Horseshoe map is chaotic on the invariant set Λ. Also note that the Smale Horseshoe map is not chaotic on the set I^2, the unit square, since periodic points are not dense in I^2 (i.e., we can find an open neighborhood in I^2 which does not contain a periodic point).

In a recent article published in the *American Mathematical Monthly* [Ref. 8], J. Banks et. al. prove the following theorem:

Theorem 4: If f: S → S is transitive and has dense periodic points, then f has sensitive dependence on initial conditions.

Proof: A sketch of the proof follows. Let x be an arbitrary point in S, and $\delta > 0$. Define the open ball centered at x of radius δ as $B_\delta(x) = \{y \in S: d(x,y) < \delta\}$. By the Triangle Inequality, it can be shown that there exists a periodic point q whose orbit, $O(q)$

is of distance at least 4δ from x. Since periodic points are dense in S, there exists a point $p \in B_\delta(x)$ which is periodic of, say, period n. There also exists a point $z \in B_\delta(x)$ such that $f^{nj}(z)$ comes within δ of one of the points in $O(q)$ for some integer j. This follows from the fact that f is transitive and requires careful construction of neighborhoods about the points in $O(q)$. Once again by way of the Triangle Inequality and the fact that $f^{nj}(p) = p$, it can be shown that $d(f^{nj}(p), f^{nj}(z)) > 2\delta$. A final application of the Triangle Inequality implies that either $d(f^{nj}(x), f^{nj}(z)) > \delta$ or $d(f^{nj}(x), f^{nj}(p)) > \delta$. Thus for any neighborhood N of x, there exists a point in N, either p or z, such that the distance between them after 'nj' iterations is greater than δ. This is exactly the definition of sensitive dependence on initial conditions. For complete details see Banks et. al. [Ref. 8].

Thus in order to show that a function f: S → S is chaotic, we need only demonstrate that periodic points are dense in S and f is topologically transitive. Theorem 4 implies that f will also have sensitive dependence on initial conditions.

For a continuous system, chaotic dynamics are usually linked to the appearance of the Smale Horseshoe map (or one of its variants) in its associated Poincaré map, giving rise to homoclinic points and orbits which can often be detected numerically. Alternatively, chaotic behavior is often described using quantitative measures such as various non-integer "dimensions" that are associated with "strange attractors." Loosely speaking, these are exotic Cantor-like limit sets which exhibit distinctive structure such as quasi-self-similarity, a property that is normally associated with "fractal" sets. We will discuss these topics in greater detail in the sections that follow.

Like chaos, no single accepted definition for a "strange attractor" exists. In fact, definitions vary quite substantially. To illustrate this variance we provide the following two definitions for a "strange attractor."

The first is provided by Rasband [Ref. 9] and is presented as a practical definition. A set A is called an **attracting set** for the dynamical system $x' = f(x)$ with flow designated by $\phi_t(x)$, if there is some neighborhood U of A such that $\phi_t(x) \in U$ for $t \geq 0$ and $\phi_t(x) \to A$ (i.e., $\|\phi_t(x) - A\| \to 0$) as $t \to +\infty$ for all $x \in U$. A **strange attractor** is then defined as an attracting set with non-integer "fractal dimension." Several measures of fractal dimension exist, some of which will be discussed in a later chapter.

Before stating the second definition from Guckenheimer-Holmes [Ref. 4] we provide some preliminary ideas. A closed invariant set Λ is **indecomposable** if for every pair of points x, y in Λ and $\varepsilon > 0$, there are points $x = x_0, x_1, \ldots, x_{n-1}, x_n = y$ and $t_1, \ldots, t_n \geq 1$ such that the distance from $\phi_{t_i}(x_{i-1})$ to x_i is smaller than ε (see Figure 19). That is, for any pair of points x and y in an indecomposable set, a "chain" of "nearby" flows can be constructed that links x to y.

The "Lebesgue measure" of a set $U \subset \mathbb{R}^n$ is a non-negative real value that can be informally described as a generalization of the notion of length, area, or volume (for n = 1,2, or 3, respectively), and in fact, reduces to this in "simple" cases. A set having positive Lebesgue measure need not however have a topological "interior" in $\mathbb{R}^n$. (For example, the Lebesgue measure of the interval $I = [0,1] \subset \mathbb{R}$ is one, while that of the rational numbers $\mathbb{Q}$ in I can be shown to be zero. From this it follows that the complement, the irrational numbers $I - \mathbb{Q}$ in [0,1], has Lebesgue measure one, even though this set contains no open intervals.) A rigorous definition lies beyond the scope of this thesis. For an in-depth discussion of measure theory, see Royden [Ref. 10].

Recall that q is a homoclinic point to a fixed point p if $q \neq p$ and if $q \in W^s(p) \cap W^u(p)$. A homoclinic point q is **transversal** if the tangent vectors to $W^s(p)$ and $W^u(p)$ do not coincide, and gives rise to a **transversal homoclinic orbit**, $\{\phi_t(q): -\infty < t < \infty\}$.

Guckenheimer-Holmes [Ref. 4] provide the following definition for a strange attractor. An **attractor** is an indecomposable closed invariant set Λ with the property that, given $\varepsilon > 0$, there is a set U of positive Lebesgue measure in an ε-neighborhood

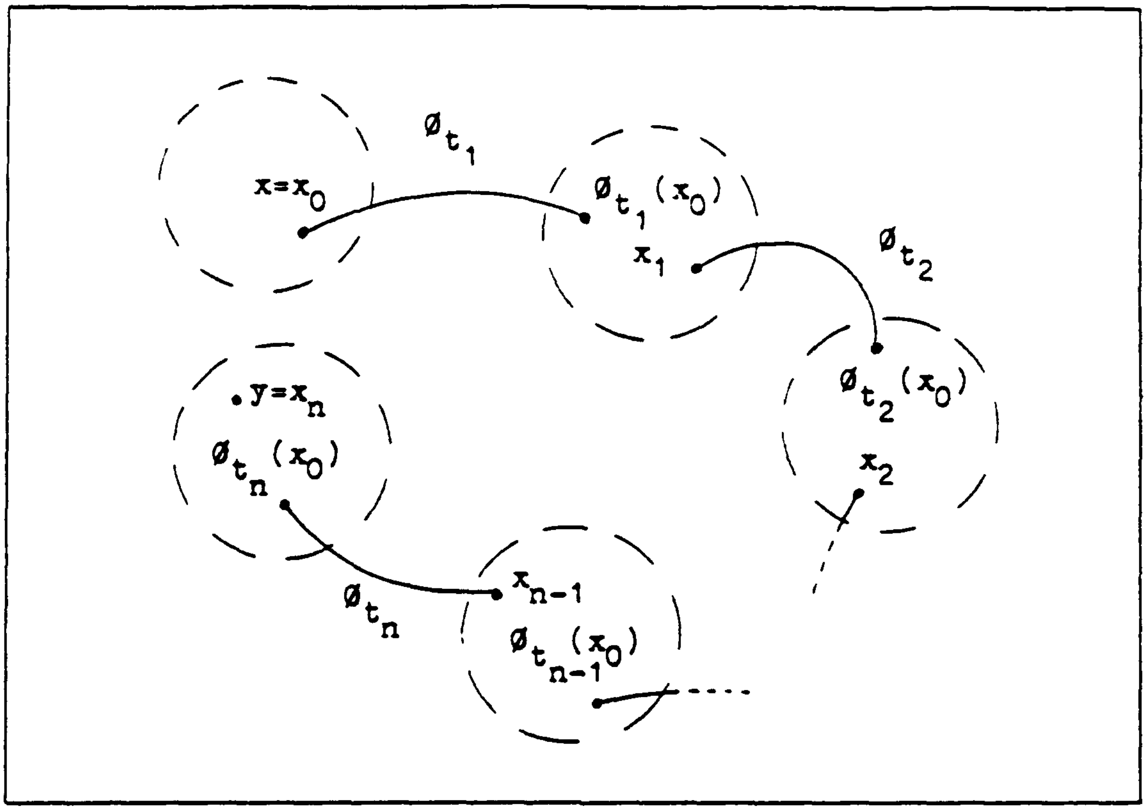

Figure 19. Schematic for an Indecomposable Set Λ

of Λ such that $x \in U$ implies that $\phi_{t_i}(x)$ for some subsequence t_i, as $t_i \rightarrow +\infty$, is contained in Λ and the forward orbit of x is contained in U. An attractor is called **strange** if it contains a transversal homoclinic orbit. This is called a **chaotic attractor** by some authors, and is consistent with the development of the notion of chaos in this thesis.

Note that the condition, "$x \in U$ implies that $\phi_{t_i}(x)$ for some subsequence t_i, as $t_i \rightarrow +\infty$, is contained in Λ ," found in the above definition is not as restrictive as the condition, "$x \in U$ implies $\phi_t(x) \rightarrow A$," found in the definition for an attracting set. It is also true however that the definition for an attracting set does not require the restriction that A be indecomposable.

Clearly these two definitions for a "strange attractor" are quite dissimilar. It should become apparent that chaos is a topic with much diversity which is yet to be unified.

The last property we will mention that is associated with a chaotic dynamical system is the existence of positive "Lyapunov exponents." A continuous or discrete system with an attracting set that has a positive Lyapunov exponent is often classified as chaotic. This property is often associated with sensitive dependence on initial conditions.

Before defining Lyapunov exponents and discussing them in-depth, we provide two examples of continuous third order autonomous systems which exhibit chaotic behavior: Duffing's equation and the Lorenz equations. It should be noted that a continuous autonomous system requires at least three dimensions in order for a strange attractor to be present. This is a direct result from the Poincaré-Bendixson Theorem which implies that an attractor for a continuous two-dimensional autonomous system can consist of only equilibrium points, periodic orbits or unions of these invariant sets (see Figure 3 for example), none of which possess a transversal homoclinic orbit or "fractal dimension." A presentation of the Poincaré-Bendixson Theorem as well as the proof can be found in Coddington-Levinson [Ref. 3]. The theorem is presented in terms of limit points and limit sets of a semi-orbit. However, two-dimensional *discrete* systems can also give rise to strange attractors, such as the Smale Horseshoe map and the Hénon map. See Peitgen-Jurgens-Saupe [Ref. 11] for examples of two-dimensional discrete systems with strange attractors.

IV. TWO EXAMPLES OF CHAOTIC SYSTEMS

A. DUFFING'S EQUATION

Duffing's equation is a second order differential equation of the form

$$x'' + cx' + bx + ax^3 = \lambda f(t) \tag{50}$$

where $'$ represents differentiation with respect to t, the coefficients a, b, c, λ are real constants (c representing damping), and $f: \mathbb{R} \to \mathbb{R}$ is a periodic forcing function with period T.

Many phenomena have been modeled by an equation of this form, including the dynamics of a buckled elastic beam and the movement of a particle in a plasma. For our discussion we will choose the constants a and b to be equal to 1 and -1 respectively. With these choices equation (50) is equivalent to the following third order autonomous system:

$$\begin{aligned} x_1' &= x_2 \\ x_2' &= x_1 - x_1^3 - cx_2 + \lambda f(t) \\ t' &= 1 \quad \bmod \mathrm{T} . \end{aligned} \tag{51}$$

We begin with the undamped unforced case: $\lambda = 0$ and $c = 0$. A Poincaré map $P: \Pi \to \Pi$ can be formulated by choosing the plane Π to be parallel to the t-axis. Specifically, let Π be the x_1, x_2 plane where $t = 0$. In this case the image of the Poincaré map is quite similar to the phase diagram for the Duffing equation (i.e., it is equivalent to sampling the phase diagram in intervals of T).

The Poincaré map has three fixed points (-1,0), (1,0) and (0,0). These fixed points correspond to periodic orbits of period T for the continuous system (51). The Jacobian matrices of P at (-1,0) and (1,0) have eigenvalues $\pm i\sqrt{3}$. The Jacobian of P at (0,0) has eigenvalues ± 1. The phase diagram and the image of the Poincaré map are shown in Figures 20 and 21. The point q in Figure 20 is a homoclinic point and the loops on either side of the point $p = (0,0)$ are homoclinic orbits.

For c some positive value and $\lambda = 0$, the fixed points for the Poincaré map remain (-1,0), (1,0) and (0,0); however only (-1,0) and (1,0) are attracting. These attracting fixed points correspond to asymptotically stable equilibrium points. The phase diagram is plotted in Figure 22.

If we keep c positive and increase the forcing parameter λ, the fixed points of the Poincaré map shift and a transversal homoclinic point emerges near (0,0). Let p be the shifted fixed point from (0,0). Figure 23 depicts the changing manifolds of p and the emergence of transversal homoclinic points as λ increases.

We now give some preliminary definitions prior to stating a special case of the Smale-Birkhoff Homoclinic Theorem, which relates the presence of a transversal homoclinic point to the shift map defined in discussing the Smale Horseshoe. A map $P: \mathbb{R}^2 \to \mathbb{R}^2$ is $\mathbf{C}^1$ if all of its first partial derivatives exist and are continuous. The map $P: \mathbb{R}^2 \to \mathbb{R}^2$ is $\mathbf{C}^\infty$ if all mixed k^{th} partial derivatives exist and are continuous for all k. A map $P: \mathbb{R}^2 \to \mathbb{R}^2$ is a **diffeomorphism** if it is one-to-one, onto and C^∞, and its inverse is also C^∞. Recall that a fixed point p of the map $P: \mathbb{R}^2 \to \mathbb{R}^2$ is **hyperbolic** if the Jacobian $DP(p)$ has no eigenvalues of unit modulus.

Theorem 5: Let $P: \mathbb{R}^2 \to \mathbb{R}^2$ be a diffeomorphism such that p is a hyperbolic point and there exists a transversal homoclinic point $q \neq p$. Then P has an invariant set Λ on which P is topologically equivalent to the shift map on Σ' (binary bi-infinite sequences).

It should be noted that the Smale-Birkhoff Homoclinic Theorem is a generalization of Theorem 5 to maps $P: \mathbb{R}^n \to \mathbb{R}^n$.

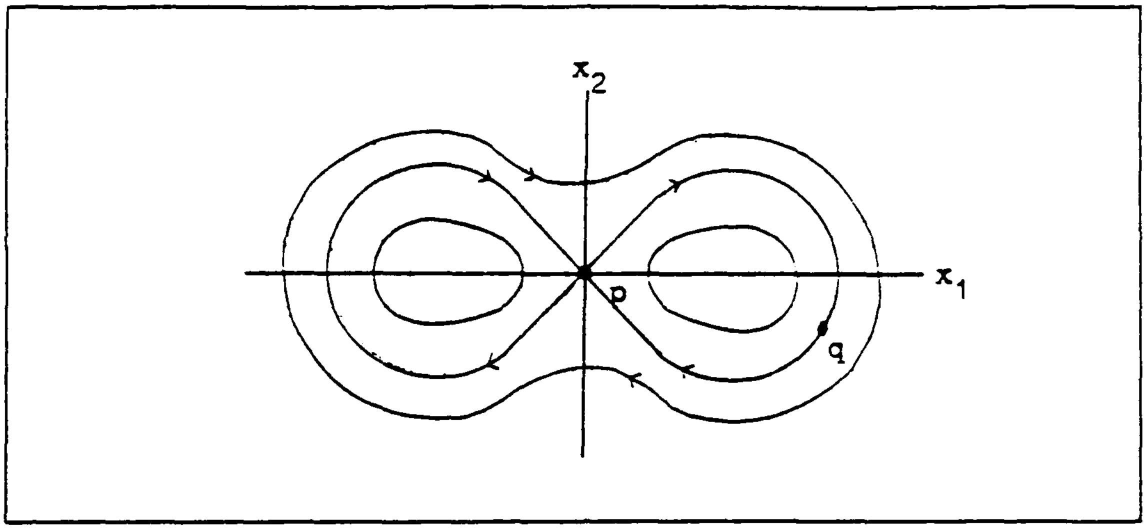

Figure 20. **Phase Diagram for $\lambda = 0$, $c = 0$.**

Proof: The proof of the Smale-Birkhoff Homoclinic Theorem is detailed in Guckenheimer-Holmes [Ref. 4]. It links the geometry of a transversal homoclinic point to that of a Smale Horseshoe map by way of Markov partitions.

We conclude from Theorem 5 that whenever the parameters are such that the Poincaré map for a continuous dynamical system, in particular Duffing's equation, has a transversal homoclinic point then in the neighborhood of such a point the map has the same properties as the Smale Horseshoe:

1. sensitive dependence on initial conditions,
2. existence of a dense orbit, which implies topological transitivity,
3. dense set of periodic points.

That is, the Poincaré map associated to Duffing's equation is chaotic whenever the parameters are such that a transversal homoclinic point is present. There has been much work done on this equation, and much ongoing research as well; see Guckenheimer-Holmes [Ref. 4].

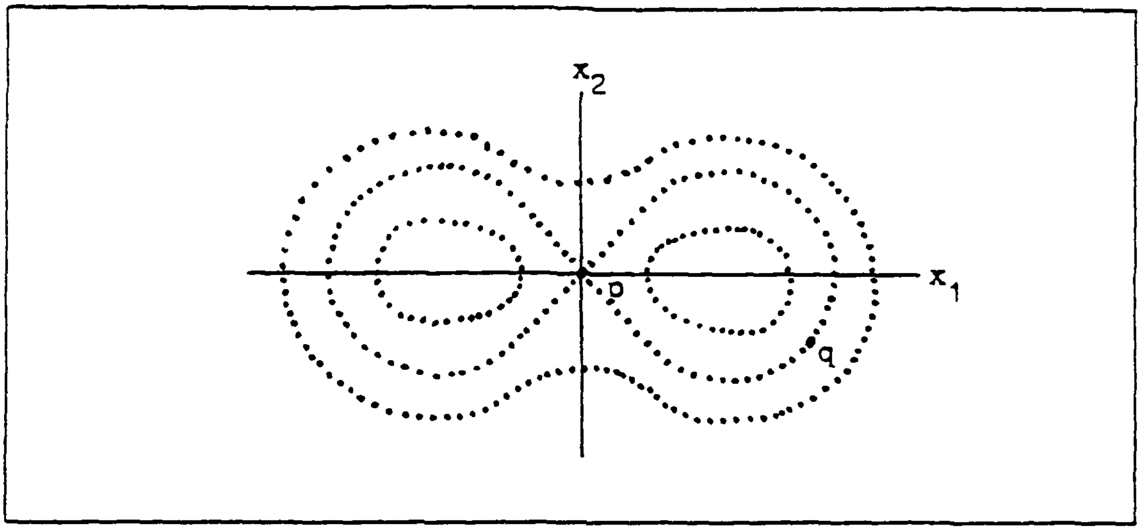

Figure 21. Image of Poincaré Map for $\lambda = 0, c = 0$.

B. LORENZ EQUATIONS

The "Lorenz equations" of meteorology are a third order autonomous system of differential equations. Formulated in an effort to model some of the unpredictable behavior associated with weather, this system has become further popularized by the chaotic dynamics it exhibits, such as the so-called "butterfly effect." It characterizes a fluid layer heated from below and cooled from above and is written in the following form:

$$
\begin{aligned}
x' &= \sigma(y - x) \\
y' &= rx - y - xz \\
z' &= xy - bz \quad .
\end{aligned}
\tag{52}
$$

The variables x, y and z represent convective motion and the horizontal and vertical temperature variations, respectively. The parameters σ (Prantl number), r (Rayleigh number), and b (an aspect ratio) are positive real constants. Although this system has been analyzed for a wide range of parameter values we shall adopt the traditional ones where $\sigma = 10$, $b = \frac{8}{3}$ and r is varied.

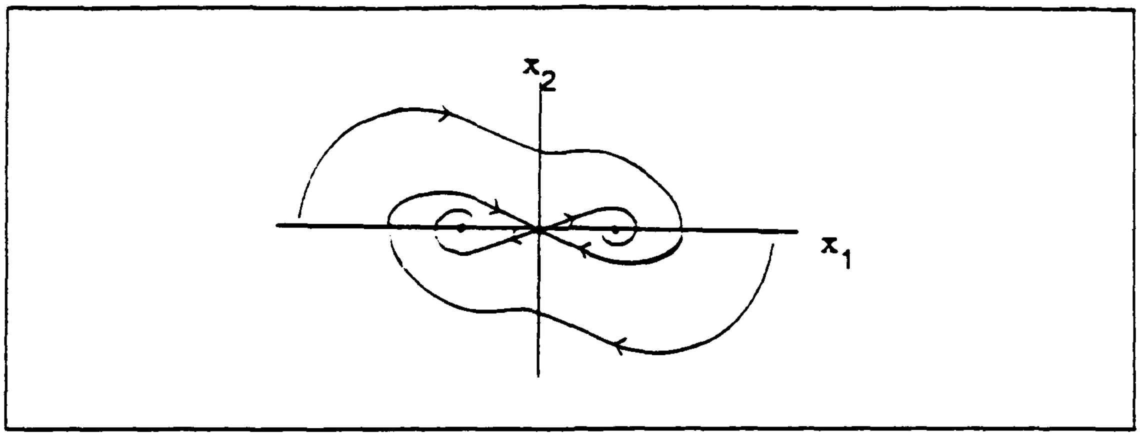

Figure 22. Phase Diagram for $\lambda = 0, c > 0$.

For $r \approx 1$ the Lorenz equations accurately model the dynamics of a convective system. For r "far" from one the equations are not an accurate model for the fluid's dynamics but have been used to model other physical systems. [Ref. 12]

We begin by presenting properties of the Lorenz equations which are true for any values of σ , r and b. First, there is a natural symmetry of variables under the transformation $(x,y,z) \rightarrow (-x,-y,z)$. That is, any dynamical behavior that occurs in a particular octant is reflected through the z-axis to the octant diagonally opposite.

Secondly, the origin is clearly an equilibrium point for the Lorenz system for all parameter values. Moreover, if an initial point $(0,0,z_0)$ is chosen, then direct inspection of the equations in (52) shows that $x'(0) = y'(0) = 0$, and $z'(0) = -bz_0$. Since z_0 is arbitrary, this shows that the z-axis $x = y = 0$ is invariant, i.e., flows which start on the z-axis stay on it, and furthermore, tend toward the origin (0,0,0). Thus the z-axis is contained in $W^s(0)$.

We will show that there exists an ellipsoid $E \subset \mathbb{R}^3$ for which the flow along the boundary is always directed inward. This implies that there exists a bounded attracting set A defined by

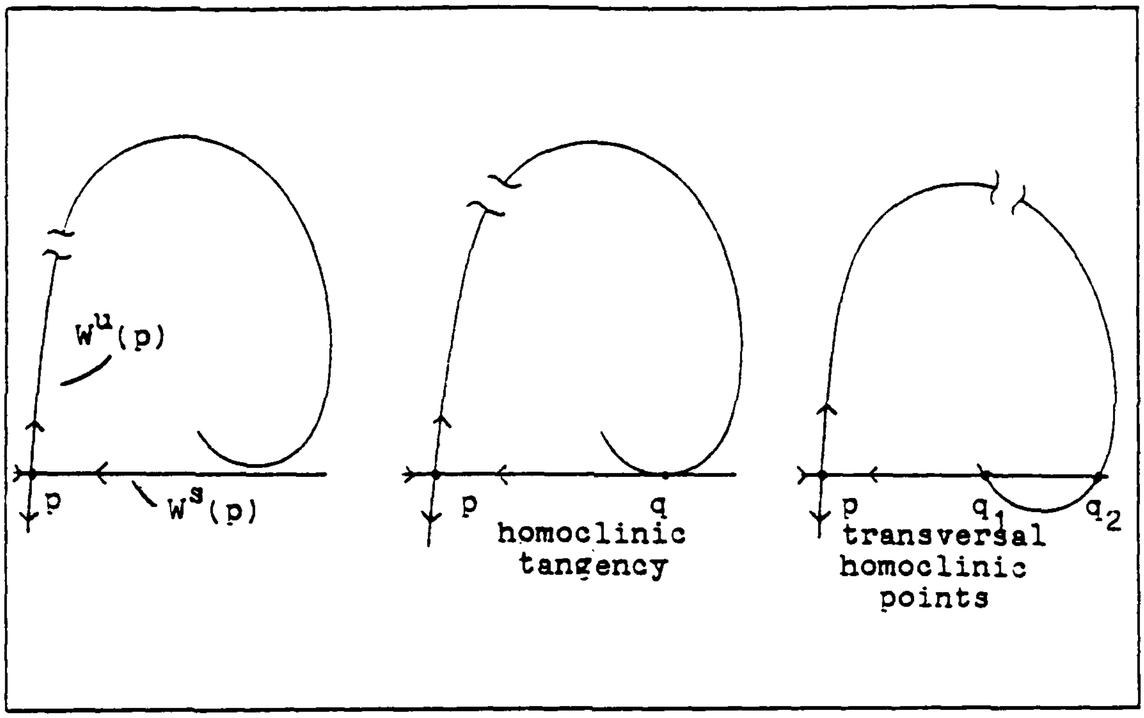

Figure 23. Emergence of Transversal Homoclinic Points.

$$A = \bigcap_{t \geq 0} \phi_t(E). \tag{53}$$

To see that such an ellipsoid E exists, consider

$$E_\mu = \{(x,y,z) \in \mathbb{R}^3 : \frac{x^2}{2\sigma} + \frac{y^2}{2} + \frac{z^2}{2} - (r+1)z - \mu = 0\} \tag{54}$$

for μ a positive constant. Showing that the dot product V of the velocity vector for (52) with the outward normal vector of E_μ is always negative implies that the flow is always directed inward along E_μ:

$$\begin{aligned} V &= x' \frac{\partial E_\mu}{\partial x} + y' \frac{\partial E_\mu}{\partial y} + z' \frac{\partial E_\mu}{\partial z} \\ &= -x^2 - y^2 - bz^2 + bz(r+1)\,. \end{aligned} \tag{55}$$

If (x,y,z) is on the ellipsoid E_μ, that is,

$$\frac{x^2}{2\sigma} + \frac{y^2}{2} + \frac{z^2}{2} - (r+1)z - \mu = 0\,, \tag{56}$$

then

$$V = (-1 + \frac{b}{2\sigma})x^2 + (-1 + \frac{b}{2})y^2 - \frac{b}{2}z^2 - b\mu \tag{57}$$

which is negative for sufficiently large μ.

Note that any ellipsoid which contains E_μ in its interior will have the flow along its boundary always directed inward. This implies that any flow starting a finite distance from the origin will stay a finite distance from the origin (i.e., no flows tend toward infinity).

The linearized system of (52) has Jacobian equal to

$$\begin{bmatrix} -\sigma & \sigma & 0 \\ r-z & -1 & -x \\ y & x & -b \end{bmatrix}. \tag{58}$$

At the origin $x = y = z = 0$, the Jacobian is

$$\begin{bmatrix} -\sigma & \sigma & 0 \\ r & -1 & 0 \\ 0 & 0 & -b \end{bmatrix}, \tag{59}$$

which has eigenvalues

$$\lambda_1, \lambda_2 = \frac{-(\sigma+1) \pm \sqrt{(\sigma-1)^2 + 4\sigma r}}{2}\,, \quad \lambda_3 = -b. \tag{60}$$

For $r < 1$ all eigenvalues of (59) are less than zero (i.e., the origin is asymptotically stable). In fact, all solutions, not just those in some small neighborhood, tend toward the origin. Note that in this case the attracting set A defined in (53) consists of only one point, namely the origin, and $W^s(0) = \mathbb{R}^3$, i.e., the origin is "global" sink. See Figure 24 for a phase diagram schematic with $r < 1$.

For $r = 1$ the eigenvalues of (59) are

$$\lambda_1 = 0, \quad \lambda_2 = -(\sigma + 1), \quad \lambda_3 = -b. \tag{61}$$

Two eigenvalues are negative and one is equal to zero. Thus for $r = 1$ the origin is no longer *asymptotically* stable but still satisfies the definition of a stable equilibrium point.

As r becomes greater than one, two additional equilibrium points $q^+ = (\sqrt{b(r-1)}, \sqrt{b(r-1)}, r-1)$ and $q^- = (-\sqrt{b(r-1)}, -\sqrt{b(r-1)}, r-1)$ appear which are initially asymptotically stable. The origin is now neither stable nor unstable for $r > 1$. This transition as the parameter passes through $r = 1$ is an example of a "bifurcation." A discussion of bifurcations for continuous systems can be found in Guckenheimer-Holmes [Ref. 4].

For $r > 1$ two eigenvalues (λ_2, λ_3) of (59) are negative and one (λ_1) is positive. By Theorem 2 of Chapter II the unstable manifold $W^u(0)$ at the origin has dimension one and $W^s(0)$ has dimension two. The eigenvalues for the Jacobian matrices evaluated at q^+ and q^- all have real parts negative when $1 < r < r_H$. (When $\sigma = 10$ and $b = \frac{8}{3}$, $r_H \approx 24.74$.) The equilibrium points q^+ and q^- are asymptotically stable. The attracting set A now consists of three points: the origin, q^+ and q^-. See Figure 25 for a schematic for r close to but greater than one.

For $1 < r < r_H$ the flow along the unstable manifold $W^u(0)$ approaches q^+ and q^-. For r-values moderately larger than one, flows which start nearer to q^+ will spiral in toward it and those which start nearer to q^- will spiral in toward that. As r increases past

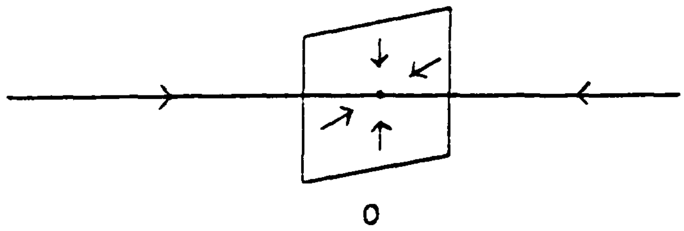

Figure 24. Phase Diagram $r < 1$.

a critical value r', the flows along the unstable manifold "cross over" and spiral in toward the "opposite" equilibrium point. (When $\sigma = 10$ and $b = \frac{8}{3}$, $r' \approx 13.926$.) At $r = r'$ homoclinic orbits exist which contain the origin. See Figures 26, 27 and 28 for schematics for $1 < r < r'$, $r = r'$ and $r' < r < r_H$ respectively.

As r is increased past r_H, the equilibrium points q^- and q^- are no longer stable. The attracting set A increases in complexity. Using a version of symbolic dynamics similar to that of the Smale Horseshoe, it is possible to show that the Lorenz equations can eventually be classified as chaotic on A through the formation of transversal homoclinic orbits. Figure 29 illustrates a numerical solution of the "Lorenz attractor," projected onto the xz-plane with $\sigma = 10$, $b = \frac{8}{3}$ and $r = 60$. It is also possible to show that A is a strange attractor, possessing non-integer "fractal dimension;" see Rasband [Ref. 9].

The Lorenz equations are filled with much richness that we have not discussed. They exhibit horseshoes, a phenomenon known as "period-doubling" and also undergo a series of "homoclinic explosions." Sparrow [Ref. 12] provides a detailed analysis of the Lorenz equations.

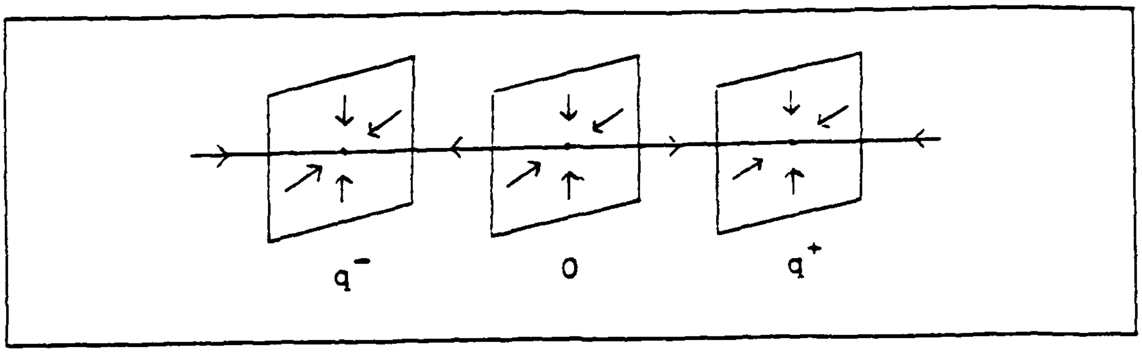

Figure 25. **Phase Diagram $r > 1$.**

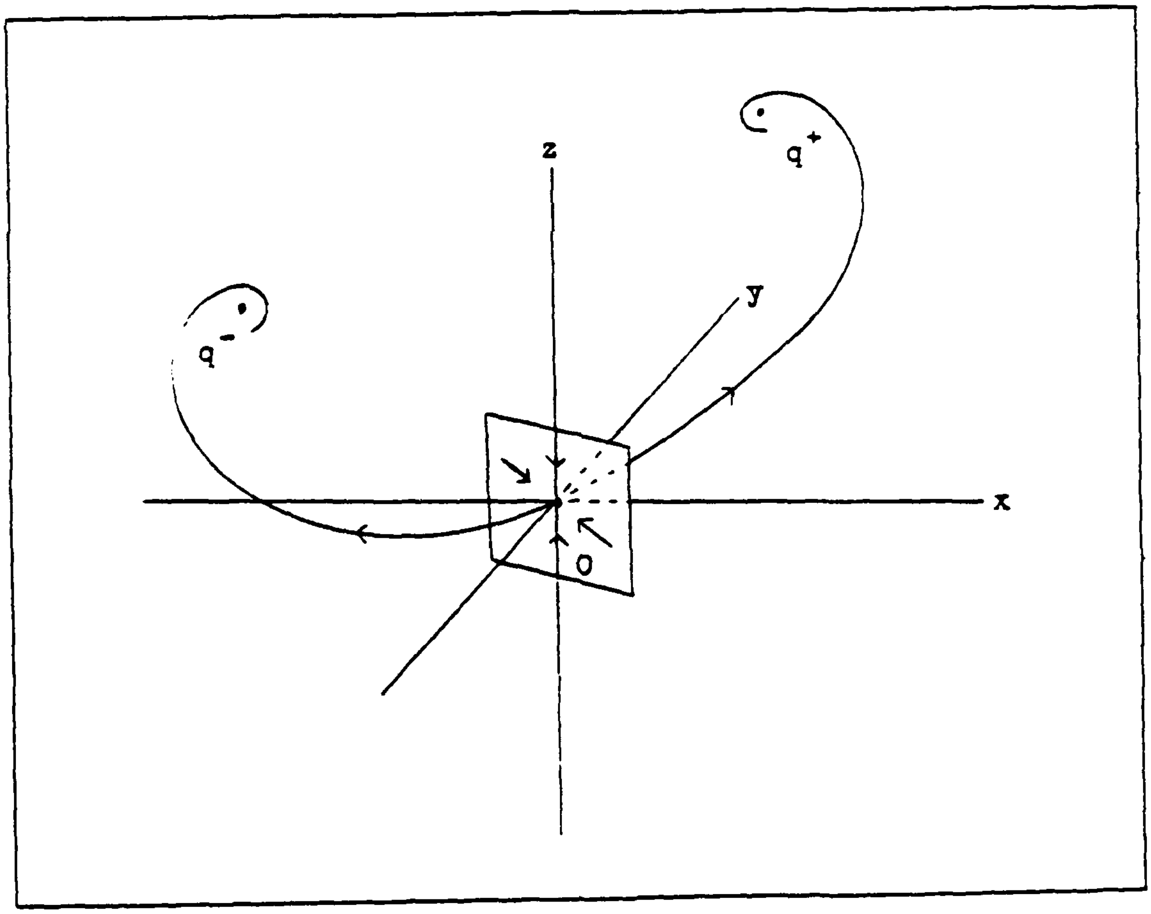

Figure 26. **Phase Diagram $1 < r < r'$.**

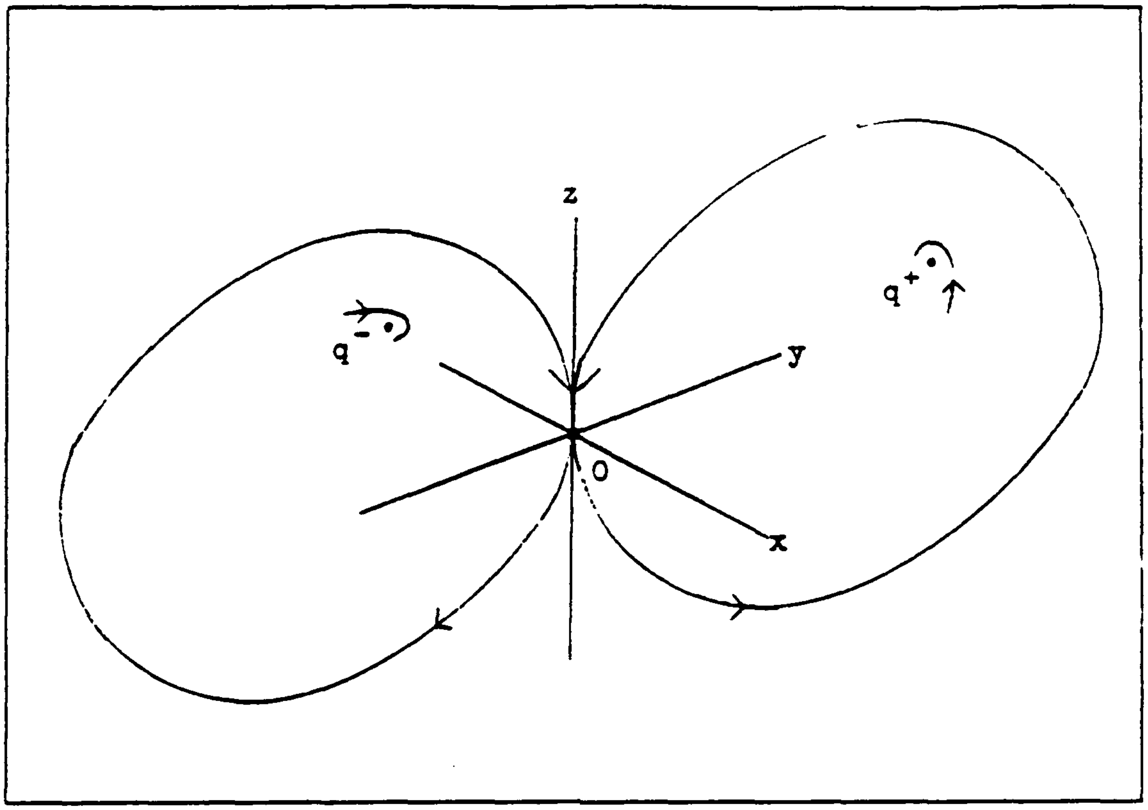

Figure 27. Phase Diagram $r = r'$.

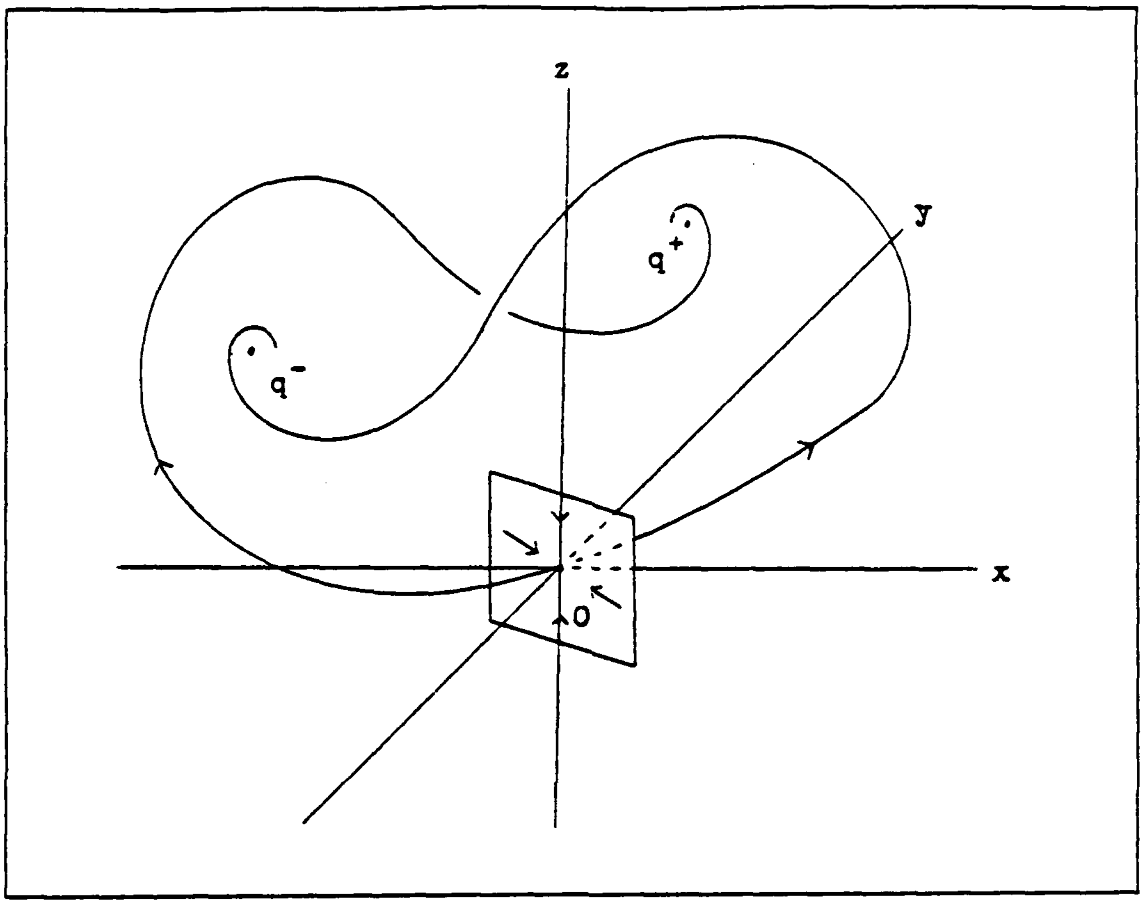

Figure 28. **Phase Diagram** $r' < r < r_H$.

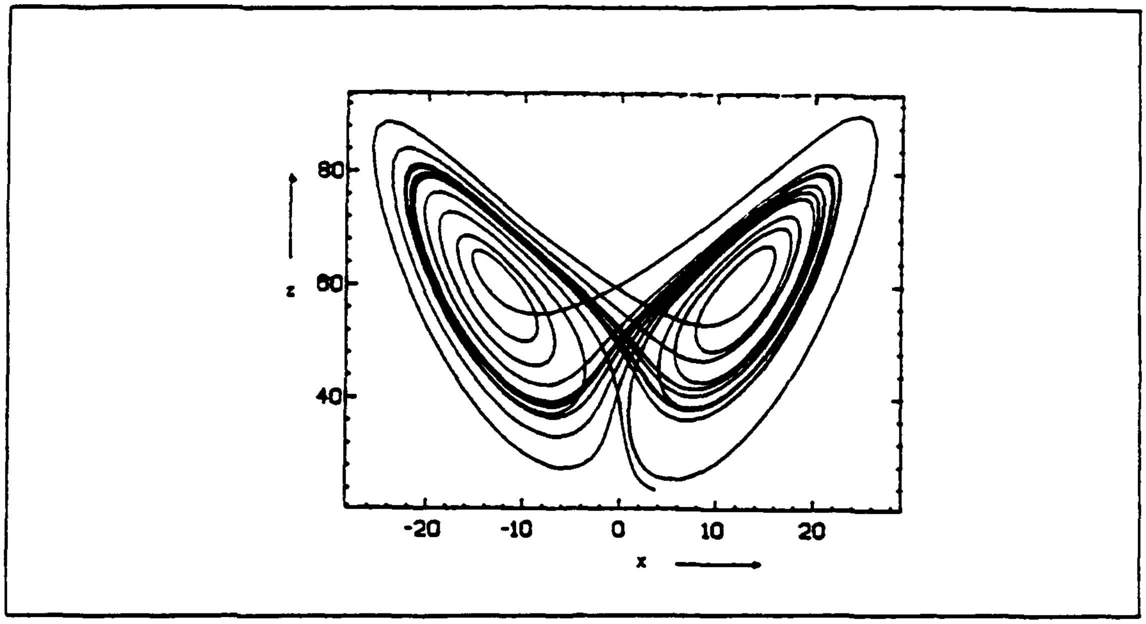

Figure 29. Numerical Solution: ($\sigma = 10, b = \frac{8}{3}, r = 60$.) Picture is from Sparrow [Ref. 12].

V. QUANTITATIVE MEASURES OF CHAOS

A. LYAPUNOV EXPONENTS

Up to now we were concerned with defining chaos and deciding whether or not a system was chaotic. Quantitative measures of chaos not only indicate when chaos is present in a dynamical system, but attempt to capture the degree of this behavior by assigning it a numerical value. Lyapunov exponents are one such quantitative measure.

Lyapunov exponents are numbers which measure the amount of exponential divergence or convergence between flows with "close" initial points, and are normally associated with a flow $\phi_t(x)$ (specifically a bounded flow such as on an attractor). Of most concern is the largest Lyapunov exponent. If the largest Lyapunov exponent of an attractor is positive then it would seem plausible that the attractor would have sensitive dependence on initial conditions. In fact many authors call a system chaotic if the largest Lyapunov exponent for an attractor is positive.

The full definition of Lyapunov exponents is somewhat involved, and the following non-rigorous argument suffices as motivation for the definition of the largest of them. Let λ be a scalar, and consider the first order autonomous differential equation $x' = \lambda x$, $x(0) = x_0$, the solution of which is $x = x_0 e^{\lambda t}$. Thus, a pair of initial points separated by a distance $d_0 > 0$ and allowed to flow from time 0 to time t eventually become separated by a distance $d(t) = d_0 e^{\lambda t}$. If $\lambda > 0$, then the flows diverge exponentially, regardless of how close they were initially.

More generally, let $\phi_t(x)$ be a bounded flow on an attractor, and let $d(t)$ represent the distance between the flow $\phi_t(x)$ and some "nearby" flow at time t. Suppose now that $d(t) = d_0(t)e^{\lambda t}$ for some "initial distance" function $d_0(t)$ and scalar λ. Then λ is said to be a **Lyapunov exponent** for the flow $\phi_t(x)$. For $k = 1,2,\ldots,N,\ldots$, as t runs from some time

t_{k-1} to a close but later time t_k, a "small" initial distance of $d_0(t_{k-1})$ between these flows is multiplied by an exponential growth factor. That is, locally,

$$d(t_k) \approx d_0(t_{k-1})e^{\lambda(t_k - t_{k-1})} \quad . \tag{62}$$

Beyond this time value of t_k, if the growth rate of $d(t)$ becomes "too large" for exponential growth, then a new "nearby" flow is chosen with a new initial distance $d_0(t_k)$, and the process is repeated; see Figure 30. The form of formula (62) suggests that

$$\lambda(t_k - t_{k-1}) \approx \ln \frac{d(t_k)}{d_0(t_{k-1})} \quad . \tag{63}$$

Summing from k = 1 to N and taking an appropriate limit yields a precise definition:

$$\lambda = \lim_{N \to \infty} \quad \frac{1}{t_N - t_0} \sum_{k=1}^{N} \ln \frac{d(t_k)}{d_0(t_{k-1})} \quad . \tag{64}$$

Thus the largest Lyapunov exponent for the flow $\phi_t(x)$ can be estimated by averaging the local expansion rates over time. Other expressions for λ exist, as well as versions for flows of discrete maps. It should be noted that the choice of the exponential e in (62) is arbitrary; base 2 is often used.

Another method for estimating the largest Lyapunov exponent for a bounded flow $\phi_t(x)$ follows. We first provide the following definitions. Let L be a matrix with complex elements l_{ij}. A matrix L^* is defined as the **Hermitian conjugate matrix** of L if the elements l^*_{ij} of L^* are equal to the complex conjugates of the elements of L transpose (i.e., $l^*_{ij} = \bar{l}_{ji}$). The **trace** of a n × n matrix L, Tr(L), is equal to the sum of its diagonal elements (i.e., $\mathrm{Tr}(L) = \sum_{i=1}^{n} l_{ii}$).

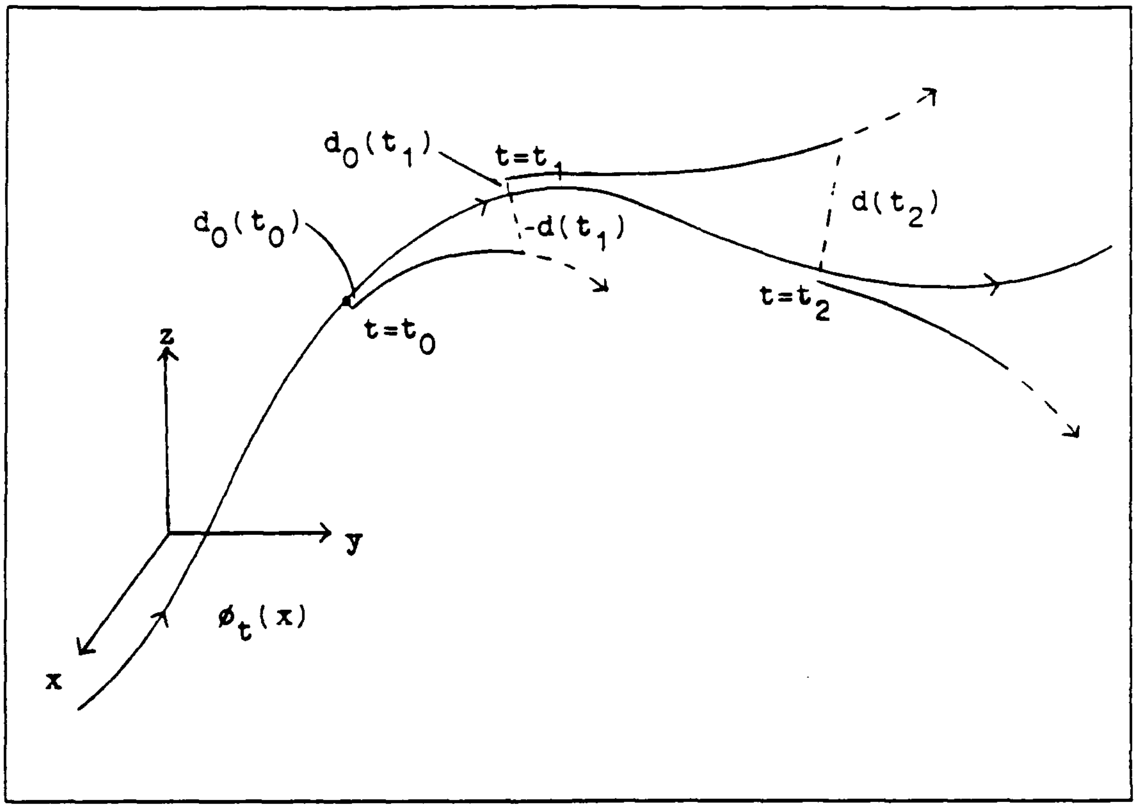

Figure 30. Estimation of a Lyapunov Exponent

Instead of defining a Jacobian matrix evaluated at a single point, consider $Df(\phi_t(x))$, a Jacobian matrix evaluated for an entire flow. It depends on the parameter t and is illustrated by the following example. Given a flow for the Lorenz equations

$$\phi_t(x) = \begin{bmatrix} x(t) \\ y(t) \\ z(t) \end{bmatrix}, \tag{65}$$

we have

$$Df(\phi_t(x)) = \begin{bmatrix} -\sigma & \sigma & 0 \\ r-z(t) & -1 & -x(t) \\ y(t) & x(t) & -b \end{bmatrix}. \tag{66}$$

It is possible to relate the distance $d(t)$ between $\phi_t(x)$ and a "nearby" flow by the following expression:

$$d'(t) = Df(\phi_t(x))d(t). \tag{67}$$

An analytic solution for $d(t)$ using (67) is virtually impossible except in some special cases. However, (67) can be integrated numerically such that

$$d(t) = L(t)d_0(t_0) \tag{68}$$

where $L(t)$ is a matrix with the same dimension as $Df(\phi_t(x))$ (i.e., $n \times n$). The largest Lyapunov exponent is the average of the eigenvalues of $L(t)$ with the largest real part as t goes from zero to infinity. Mathematically, for λ the largest Lyapunov exponent,

$$\lambda = \lim_{t \to \infty} \frac{1}{2t} \ln[\mathrm{Tr}(L^{+}(t)L(t))] \tag{69}$$

where L^{+} is the Hermitian conjugate matrix of L and $\mathrm{Tr}(L^{+}(t)L(t))$ is the trace of the matrix product $L^{+}(t)L(t)$. The limit in (69) has been established by "multiplicative ergodic theorems" to exist for a large category of systems.

It should be noted that an entire spectrum of Lyapunov exponents exists, largest to smallest. In general, for an n^{th} order autonomous system there are n Lyapunov exponents. The spectrum of Lyapunov exponents for an equilibrium point p of the system $x' = f(x)$ consists of exactly the real parts of the eigenvalues of the Jacobian $Df(p)$.

For an attractor to exist it must be true that the sum of the Lyapunov exponents is negative. It can also be shown that for a system $x' = f(x)$, if $\phi_t(x)$ is bounded for $t \geq 0$, if $\phi_t(x)$ does not tend toward an equilibrium point, and if f has a finite number of zeros, then at least one of the Lyapunov exponents for $\phi_t(x)$ is zero; see Parker-Chua [Ref. 7].

With the last two statements in mind the only possible spectrum of Lyapunov exponents $(\lambda_1, \lambda_2, \lambda_3)$ for a three-dimensional system with an attractor is one where $\lambda_1 > 0$, $\lambda_2 = 0$, $\lambda_3 < 0$ and $\lambda_1 < -\lambda_3$.

B. FRACTAL DIMENSION

Fractal dimensions are dimensions which allow non-integer values. The dimension of Euclidean space is the dimension with which we are most familiar and is not considered a fractal dimension. It assigns only integer-valued dimensions; a point has dimension zero, a line dimension one, a plane dimension two, and a cube dimension three. Fractal dimensions are consistent with the dimension of Euclidean space in that a point, line, plane and cube all have the appropriate integer valued dimensions.

We are most concerned with defining an appropriate dimension for invariant sets, in particular, strange attractors. Note that we have already seen that strange attractors can be defined as attracting sets with non-integer fractal dimension. Inasmuch as most (but not all) strange attractors exhibit chaos in the sense of possessing transversal homoclinic orbits (and thus sensitive dependence on initial conditions, etc.), the dimensions of non-chaotic attractors are always integers.

We start with a notion of fractal dimension called capacity. Given an attractor Λ, cover it with appropriate volume elements (i.e., spheres, cubes, circles, squares, intervals, etc.) each with diameter ε. Let $N(\varepsilon)$ denote the number of volume elements with diameter ε needed to cover Λ. As ε decreases the number of volume elements $N(\varepsilon)$ needed to cover Λ increases, that is,

$$N(\varepsilon) = c\varepsilon^{-D} \tag{70}$$

for some constants c, and D. The **capacity** D_{cap} is derived by solving (70) for D and letting ε approach zero, that is,

$$D_{cap} = \lim_{\varepsilon \to 0} \frac{\ln N(\varepsilon)}{\ln(\frac{1}{\varepsilon})} \tag{71}$$

provided the limit exists independent of the shape of the boxes used to compute $N(\varepsilon)$. If the limit does not exist, the capacity is undefined. Capacity is also known as **box** or **box-counting** dimension.

Consider the capacity for the unit square. Let the volume elements be boxes with sides of length $\varepsilon = \frac{1}{3^k}$. If k = 1 then nine boxes are necessary to cover the unit square. For k = 2, eighty-one boxes are necessary. In general $N(\varepsilon) = 3^{2k}$ boxes are necessary to cover the unit square. Letting $\varepsilon \to 0$ is equivalent to letting $k \to \infty$, thus

$$D_{cap} = \lim_{k \to \infty} \frac{\ln 3^{2k}}{\ln 3^k} = 2\,. \tag{72}$$

Notice that two is consistent with the Euclidean dimension for the unit square.

Now consider the Cantor Ternary set briefly introduced in Chapter III. This set is a subset of the unit interval and thus the appropriate volume elements will be intervals. After completion of the first step in our construction of the Cantor Ternary set we were left with two intervals $[0, \frac{1}{3}]$, $[\frac{2}{3}, 1]$. These intervals can be covered with two intervals of length one-third. In general after the k^{th} step, $N(\varepsilon) = 2^k$ intervals of length $\varepsilon = \frac{1}{3^k}$ are sufficient to cover the resulting set. Thus the capacity of the Cantor Ternary set is

$$D_{cap} = \lim_{k \to \infty} \frac{\ln 2^k}{\ln 3^k} = \frac{\ln 2}{\ln 3} \approx 0.6309\,. \tag{73}$$

Notice that D_{cap} is not an integer and that the value is less than the dimension of the unit interval (dimension one) of which the Cantor Ternary set is a subset.

In calculating the capacity for attractors such as those found for Duffing's equation and the Lorenz equations, note that equation (70) can be written as

$$\ln N(\varepsilon) = D(\ln(\tfrac{1}{\varepsilon})) + \ln c \ . \qquad (74)$$

Thus, in a limiting sense, D_{cap} is the slope of the log-log plot of $N(\varepsilon)$ versus $\frac{1}{\varepsilon}$.

$N(\varepsilon)$ can be calculated for an appropriate number of different ε-values by constructing a grid of boxes (hyper-cubes) with sides of length ε that cover an area (n-dimensional phase space) which bounds the attractor. For Duffing's equation, $n=2$, and boxes are used for volume elements. For the Lorenz equations, $n=3$, and cubes are used for volume elements. This grid of boxes (hyper-cubes) can be initialized in a boolean array with value FALSE. For each data point x_i on the attractor determine in which box it is contained and change the corresponding array value to TRUE. $N(\varepsilon)$ is the number of elements in the array which are marked TRUE.

It should be noted that for n greater than three, computer memory requirements become excessive. In this case other more efficient methods (see Parker-Chua [Ref: 7]) can be used for calculating D_{cap}. Additionally the number of data points x_i on the attractor used in calculating the capacity as well as the other fractal dimensions is critical. We will return to this issue at the end of the section.

The next measure we shall discuss is called the information dimension. We maintain the notation that $N(\varepsilon)$ is the number of volume elements of diameter ε which covers the attractor. The information dimension is based on the relative frequency that the attractor "visits" any particular volume element. Let P_i be the relative frequency with which the attractor enters the i^{th} volume element. Define

$$H(\varepsilon) = -\sum_{i=1}^{N(\varepsilon)} P_i \ln P_i . \qquad (75)$$

The **information dimension** is defined by

$$D_I = \lim_{\varepsilon \to 0} \frac{H(\varepsilon)}{\ln\left(\frac{1}{\varepsilon}\right)} . \qquad (76)$$

Again if the limit does not exist D_I is undefined.

Consider the information dimension for the unit square with uniform probability density. Then as seen earlier $N(\varepsilon) = 3^{2k}$ boxes with sides of length $\varepsilon = \frac{1}{3^k}$ are necessary to cover the unit square. Since the probability density is uniform, the probability that a point chosen at random from the unit square is in a box with side of length $\varepsilon = \frac{1}{3^k}$ is equal to $\frac{1}{3^{2k}}$ (i.e., $P_i = \frac{1}{3^{2k}}$). Thus

$$H(\varepsilon) = -\sum_{i=1}^{3^{2k}} \frac{1}{3^{2k}} \ln\left(\frac{1}{3^{2k}}\right) = \ln 3^{2k} \qquad (77)$$

and the information dimension is

$$D_I = \lim_{k \to \infty} \frac{\ln 3^{2k}}{\ln 3^{k}} = 2 . \qquad (78)$$

Notice that D_I for the unit square with uniform probability is equal to D_{cap} for the unit square. In fact it is always true that $D_{cap} = D_I$ for uniform densities.

Next consider a unit square with uniform probability density equal to $\frac{1}{2}$ and the single point (2,0) with probability $\frac{1}{2}$. If the volume elements are again boxes with sides of length $\varepsilon = \frac{1}{3^k}$, then $N(\varepsilon) = 3^{2k} + 1$ boxes are necessary to cover the unit square plus the point (2,0). $P_i = \frac{1}{2}$ for the volume element covering the point (2,0) and $P_i = \frac{1}{2}\left(\frac{1}{3^{2k}}\right)$ for the remaining 3^{2k} volume elements. Thus

$$
\begin{aligned}
H(\varepsilon) &= -\frac{1}{2}\ln\frac{1}{2} - \sum_{i=1}^{3^{2k}} \frac{1}{2 \cdot 3^{2k}} \ln\left(\frac{1}{2 \cdot 3^{2k}}\right) \\
&= \frac{1}{2}\ln 2 + \frac{1}{2}\ln(2 \cdot 3^{2k}) \qquad (79) \\
&= \ln 2 + \frac{1}{2}\ln 3^{2k}
\end{aligned}
$$

and

$$
D_I = \lim_{k\to\infty} \left(\frac{\ln 2}{\ln 3^k} + \frac{\ln 3^{2k}}{2\ln 3^k}\right) = 1\,. \qquad (80)
$$

Thus D_I is the average of the dimensions of the point and the unit square. This illustrates how the information dimension can weigh the lower-dimensional subsets according to their relative frequency of "visitation," where as capacity tends to ignore the lower-dimensional subsets. It can be shown for any attractor that $D_I \leq D_{cap}$.

The final fractal dimension which we shall discuss is the correlation dimension. Keeping the same notation used for information dimension, the **correlation dimension** D_{corr} is defined by

$$
D_{corr} = \lim_{\varepsilon\to 0} \frac{\ln \sum_{i=1}^{N(\varepsilon)} P_i^2}{\ln \varepsilon}\,. \qquad (81)
$$

As an aid to interpreting the numerator of (81), let N be the number of points x_i of the attractor used to estimate D_{corr}. It is rather easy to show that for

$$C(\varepsilon) = \lim_{N\to\infty} \frac{1}{N^2} \left\{ \begin{array}{l} \text{the number of pairs of points} \\ \{x_i, x_j\} \text{ such that } \|x_i - x_j\| < \varepsilon \end{array} \right\} \tag{82}$$

(81) is equivalent to

$$D_{corr} = \lim_{\varepsilon\to 0} \frac{\ln C(\varepsilon)}{\ln \varepsilon} . \tag{83}$$

Once again consider the unit square and a single point. Let the volume elements be boxes with sides of length $\varepsilon = \frac{1}{3^k}$. Then $N(\varepsilon) = 3^{2k} + 1$. Let $P_i = \frac{1}{2}\left(\frac{1}{3^{2k}}\right)$ for the volume elements covering the unit square and $P_i = \frac{1}{2}$ for the single point. Then

$$\begin{aligned} \ln \sum_{i=1}^{N(\varepsilon)} P_i^2 &= \ln\left[\frac{1}{4} + \sum_{i=1}^{3^{2k}} \frac{1}{4 \cdot 3^{4k}}\right] \\ &= \ln\left[\frac{1}{4}\left(1 + \frac{1}{3^{2k}}\right)\right] \end{aligned} \tag{84}$$

which implies

$$\begin{aligned} D_{corr} &= \lim_{k\to\infty} \frac{\ln\left[\frac{1}{4}\left(1 + \frac{1}{3^{2k}}\right)\right]}{\ln\left(\frac{1}{3^k}\right)} \\ &= 0 . \end{aligned} \tag{85}$$

Thus the correlation dimension completely ignores the unit square in this example. It can be shown that $D_{corr} \leq D_I \leq D_{cap}$ for any attractor.

Other similar types of fractal dimensions exist which are also designed to reflect various statistical properties of the attractor. Related measures include entropy, Hausdorff dimension, and Lyapunov dimension which requires the values for the entire spectrum of Lyapunov exponents. This probabilistic approach to analyzing dynamical systems has played an important role in the development of a formal discipline known as **ergodic theory,** which relies heavily on the classical theory of measure and integration. The main reason for choosing one fractal dimension over another is the ease and accuracy of calculation, as well as computational stability and robustness. Since this area is still undergoing much active research it is unclear which dimensions are preferable and how they are related to one another. It is unlikely that the complexity of a strange attractor will ever be represented by a single number.

Much of the power in determining an attractor's fractal dimension is realized when working with data from experimental observations (i.e., time series). This provides an estimate of the minimum number of variables needed to model the systems' underlying dynamics. For example, if the dimension of the attractor is 2.7 then theoretically the underlying system can be modeled with three variables.

This leads to two questions:

1. How reliable is computational simulation of the true orbits?
2. How much data is necessary to estimate the fractal dimension of an attractor?

The first question is answered by the **Shadowing Lemma,** see Guckenheimer-Holmes [Ref. 4], which states that a computed "pseudo-orbit" does approximate some true orbit in a hyperbolic invariant set Λ. The second question is answered (specifically for correlation dimension estimated by the widely used Grassenberger-Procaccia algorithm) in Ruelle [Ref. 13]. Let N be the number of points on the attractor or number of experimentally observed data points used to estimate the correlation dimension. It can be argued that in order for the correlation dimension to be estimated accurately by this algorithm the following relation must hold:

$$\text{correlation dimension} \leq 2\log_{10} N . \tag{86}$$

Thus if the correlation dimension is estimated to be 3.7 for a certain attractor then we should ensure that substantially more than 71 data points were used in the estimation. Although the relation in (86) is specific to a fractal dimension calculated by a certain algorithm, the result suggests we should in general be wary of any fractal dimension estimated with a "small" number of data points.

APPENDIX - NOTATION

We provide the following definitions for some of the fundamental mathematical notation used in this thesis.

1. $a \in A$ - a is a member of set A
2. $\mathbb{R}$ - the set of real numbers
3. $\mathbb{R}^n$ - the set of n-tuples $(x_1, ..., x_n)$, where $x_i \in \mathbb{R}$, i = 1,...,n
4. $\mathbb{Z}$ - the set of integers, $\{0, \pm 1, \pm 2, ...\}$
5. $\mathbb{Z}^+$ - the set of non-negative integers, $\{0, 1, 2, ...\}$
6. $\mathbb{Q}$ - the set of rational numbers, $\{ \frac{m}{n} : m,n \in \mathbb{Z}, n \neq 0\}$
7. $f: A \to B$ - a function f with set A as its domain and set B as its range
8. $h \circ f$ - composition of functions, $h \circ f(x) = h(f(x))$
9. Re$\{\lambda\}$ - the real part of the complex number λ
10. Im$\{\lambda\}$ - the imaginary part of the complex number λ

LIST OF REFERENCES

1. Beaver, Philip Frederick, *Fractals and Chaos*, Masters Thesis, Naval Postgraduate School, Monterey, California, June 1991.

2. Borrelli, Robert L., and Courtney S. Coleman, *Differential Equations: A Modeling Approach*, Prentice-Hall, Inc., 1987.

3. Coddington, Earl A., and Norman Levinson, *Theory of Ordinary Differential Equations*, McGraw-Hill Book Company, Inc., 1955.

4. Guckenheimer, John, and Philip Holmes, *Nonlinear Oscillations, Dynamical Systems, and Bifurcations of Vector Fields*, Springer-Verlag, 1983.

5. Boyce, William E., and Richard C. DiPrima, *Elementary Differential Equations and Boundary Value Problems*, John Wiley & Sons, 1986.

6. Devaney, Robert L., *An Introduction to Chaotic Dynamical Systems*, Addison-Wesley Publishing Company, Inc., 1989.

7. Parker, T.S., and L.O. Chua, *Practical Numerical Algorithms for Chaotic Systems*, Springer-Verlag, 1989.

8. Banks, J. et. al., "On Devaney's Definition of Chaos," Volume 99, American Mathematical Monthly, April 1992.

9. Rasband, S. Neil, *Chaotic Dynamics of Nonlinear Systems*, John Wiley & Sons, 1990.

10. Royden, H.L., *Real Analysis*, Macmillan Publishing Company, 1988.

11. Peitgen, Heinz-Otto, Hartmut Jurgens and Dietmar Saupe, *Chaos and Fractals: New Frontiers of Science*, Springer-Verlag, 1992.

12. Sparrow, Colin, *The Lorenz Equations: Bifurcations, Chaos, and Strange Attractors*, Springer-Verlag, 1982.

13. Ruelle, D., "Deterministic Chaos: The Science and the Fiction," Volume 427, 241-248, Proc. R. Soc. London A, 1990.

INITIAL DISTRIBUTION LIST

		No. Copies
1.	Defense Technical Information Center Cameron Station Alexandria, VA 22304-6145	2
2.	Library, Code 52 Naval Postgraduate School Monterey, CA 93943-5002	2
3.	Professor I. Fischer, Code MA Fi Department of Mathematics Naval Postgraduate School Monterey, CA 93943-5000	1
4.	Professor J. Leader, Code MA Le Department of Mathematics Naval Postgraduate School Monterey, CA 93943-5000	1
5.	Department Chairman, Code MA Fe Department of Mathematics Naval Postgraduate School Monterey, CA 93943-5000	1
6.	Fontana, Tony LT, USN 1290 5th St. #1 Monterey, CA 93940	1
7.	Dyar, Walter MAJ, USMC 19 Revere Rd. Monterey, CA 93940	1
8.	Bernhard, Winfried P.O. Box 313 Maineville, OH 45039	1
9.	Bernhard, Michael LT, USN P.O. Box 313 Maineville, OH 45039	1
10.	Aissen, Michael 5 Villanova Ct. Seaside, CA 93955	1